USE OF SEAWATER AS THE MIX WATER FOR CONCRETE

by

Senem Bilici

B.S., Civil Engineering, Istanbul University, 2015

Submitted to the Institute for Graduate Studies in
Science and Engineering in partial fulfillment of
the requirements for the degree of
Master of Science

Graduate Program in Civil Engineering

Boğaziçi University

2019

ACKNOWLEDGEMENTS

I would like to express my sincere appreciation to my thesis supervisor Assoc. Prof. Nilüfer Özyurt Zihnioğlu for her kindness, cheerful face, invaluable support, encouragement and advice throughout the duration of the thesis and also i would like to thank Dr. Abdullah Huzeyfe Akça for his insightful comments and suggestions.

I am very grateful to my friend and Boğaziçi University assistant Olcay Gürabi Aydoğan, and our Construction Material Laboratory fellow, Ümit Melep for his help during our experiments.

I would like to thank BAP committee for financial support of the project 14861P.

I dedicate this thesis to myself for my endless patience. I would like to manifest my special thanks to my sister, Özlem Bilici, my father and my mother for their endless support, encouragement and love they have given me throughout my life.

ABSTRACT

USE OF SEAWATER AS THE MIX WATER FOR CONCRETE

According to the United Nations World Water Development Report in 2018, the global demand for water has been increasing at a rate of about 1% per year over the past decades as a function of population growth and economic development, and it will continue to increase dramatically in the near future. In line with these estimates, researchers in many countries of the world focused on issues such as wastewater management and widespread use of seawater within the scope of sustainability. Since concrete is the most widely used building material in the world, construction sector is among the sectors that use significant amounts of water.

Using seawater in the mixture as the mix water is potentially favorable from a sustainability viewpoint. However, the presence of high concentrations of chloride in the seawater can cause corrosion of steel reinforcement. This issue can be addressed by using non-corrosive synthetic structural fibers. This thesis reports on the results of an experimental study to compare the fresh and hardened properties of tap water and seawater-mixed concretes. The experimental program included the following tests: (a) fresh concrete test (slump flow and density); (b) mechanical tests of hardened concrete (compressive strength test, modulus of elasticity test, three - point bending test and length change test); and (c) microstructural analyses of hardened concrete (SEM/EDAX observations and X-Ray Diffraction analyses). No pronounced change was seen in mechanical performance of seawater concrete. Scanning electron microscopy and XRD analyses were used to better explain the experimental observations.

ÖZET

DENİZ SUYUNUN BETONDA KARIŞIM SUYU OLARAK KULLANIMI

Birleşmiş Milletler Dünya Su Gelişim Raporu 2018'e göre, suya olan küresel talep nüfus artışı ve ekonomik kalkınmanın bir fonksiyonu olarak son on yıldır kişi başına 1% oranında artmaktadır. Bu oran yakın gelecekte de çarpıcı bir şekilde artmaya devam edecektir. Bu tahminlere paralel olarak, dünyanın birçok ülkesindeki araştırmacılar, atık su yönetimi ve deniz suyunun sürdürülebilirlik kapsamında yaygın kullanımı gibi konulara odaklanmıştır. Özellikle beton, dünyada en çok kullanılan inşaat malzemesi olduğundan, inşaat sektörü önemli miktarda su kullanan sektörler arasına girmektedir. Betonda karışım suyu olarak deniz suyunun kullanılması, sürdürülebilirlik bakış açısından potansiyel olarak avantajlıdır. Ancak deniz suyunda yüksek konsantrasyonlarda klorür bulunması, çelik donatıda korozyona sebep olabilir. Bu sorun paslanmayan sentetik yapısal elyaflar kullanılarak giderilebilir. Bu tez kapsamında, musluk suyu ve deniz suyu ile karıştırılmış betonların, taze ve sertleşmiş hal özelliklerini karşılaştırmak için deneysel çalışmalar yapılmıştır. Deneysel program aşağıdaki testleri içermektedir: (a) taze beton testi (çökme deneyi ve yoğunluğu); (b) sertleşmiş betonun mekanik testleri (basınç dayanımı testi, elastisite modülü testi, üç noktalı eğilme testi ve uzunluk değişim testi); ve (c) sertleşmiş betonun mikroyapı analizleri (SEM/EDAX gözlemleri ve X-Işını Kırınımı (XRD) analizleri). Deniz suyu kullanılarak yapılan betonunun mekanik performansında belirgin bir değişiklik görülmedi. Deneysel gözlemleri daha iyi açıklamak için taramalı elektron mikroskobu ve XRD analizleri kullanılmıştır.

TABLE OF CONTENTS

ACKNOWLEDGEMENTS . . . iii
ABSTRACT . . . iv
ÖZET . . . v
LIST OF FIGURES . . . viii
LIST OF TABLES . . . xii
1. INTRODUCTION . . . 1
2. LITERATURE REVIEW . . . 2
2.1. Effects of Seawater as Mixing Water in Concrete . . . 3
2.2. Effect of Mineral Additives on Concretes Produced by using Seawater as the Mix Water . . . 3
2.3. Durability . . . 7
2.4. Using Synthetic Structural Fibers in Concrete . . . 8
2.5. Differences of the Microstructure . . . 10
2.6. Effects of Seawater on Shrinkage Strain of Concrete . . . 13
3. EXPERIMENTAL STUDY . . . 16
3.1. Materials . . . 16
3.1.1. Cement . . . 16
3.1.2. Admixtures . . . 18
3.1.3. Aggregates . . . 18
3.1.3.1. Sieve Analysis of Aggregates . . . 18
3.1.4. Water . . . 21
3.1.5. Fiber . . . 21
3.2. Mix Proportions . . . 23
3.2.1. Specimen Curing . . . 24
3.2.2. Number of Specimens . . . 24
3.3. Experimental Methods . . . 25
3.3.1. Fresh State Tests . . . 25
3.3.2. Hardened State Tests . . . 25
3.3.2.1. Compressive Strength Tests . . . 25

3.3.2.2. Modulus of Elasticity Tests 25
3.3.2.3. Three - Point Bending Test 28
3.3.2.4. Length Change Tests 29
3.3.2.5. Microstructural Analyses 29
4. RESULTS AND DISCUSSION 32
4.1. Fresh Concrete Properties 32
4.2. Hardened Concrete Properties 32
4.2.1. Compressive Strength Analysis 32
4.2.2. Modulus of Elasticity Test Results 35
4.2.3. Three - Point Bending Test Results 36
4.2.4. Length Change Test Results 40
4.2.5. SEM / EDAX Observations 41
4.2.6. XRD Results 49
5. CONCLUSION 54
REFERENCES 56

LIST OF FIGURES

Figure 2.1. Number of articles published from 1974 to 2013 on the use of seawater as the mixing water in concrete [3] 2

Figure 2.2. Compressive strength of concrete [6] 4

Figure 2.3. 28th day compressive strength with replacement fly ash and GGBFS in normal water (NW) and seawater (SW) [8] 5

Figure 2.4. 28th - day tensile strength with replacement fly ash and GGBFS in normal water (NW) and seawater (SW) [8] 6

Figure 2.5. Modulus of elasticity for a) macro - polymeric fiber-reinforced concrete, b) polypropylene fiber-reinforced concrete [12] 9

Figure 2.6. Splitting tensile strength for: a) macro - polymeric fiber-reinforced concrete, b) polypropylene fiber-reinforced concrete [12] 9

Figure 2.7. SEM images of mortars for: a) tap water + CN + silica fume (SF), b) seawater + CN + silica fume (SF) [6] 10

Figure 2.8. XRD intensity of ettringite in the concrete [6] 11

Figure 2.9. XRD result of the non-MK + seawater mix (P7) and MK+seawater mix (P11) [9] 12

Figure 2.10. Length change ratio owing to drying shrinkage [6] 13

Figure 2.11. Drying shrinkage of concretes (Mix A : Reference cement+fly ash+fresh water, Mix B: Seacon cement+ fly ash+fresh water, Mix C: Reference cement+fly ash+seawater, Mix D: Reference cement+fly ash+fresh water+RCA) [15] 14

Figure 2.12. Shrinkage test results [2] 15

Figure 3.1. Gradation curve of the mixture 20

Figure 3.2. Structural macro - synthetic fibers 22

Figure 3.3. Loading procedure for the determination of initial and stabilized secant modulus of elasticity [27] 26

Figure 3.4. Modulus of elasticity test setup 27

Figure 3.5. Three - point bending test setup 28

Figure 3.6. Sampling locations for SEM analysis 30

Figure 3.7. A test sample of fibrous-concrete for ESEM / EDAX analysis . . . 31

Figure 4.1. Compressive strength of non-fibrous specimens 33

Figure 4.2. Compressive strength of fibrous specimens 34

Figure 4.3. Modulus of elasticity of non - fibrous specimens 35

Figure 4.4. Modulus of elasticity of fibrous specimens 36

Figure 4.5. Calculation of area under the curve 37

Figure 4.6. Force – CMOD graphs of non - fibrous specimens 38

Figure 4.7. Force – CMOD graphs of fibrous specimens 39

Figure 4.8. Length change ratio of non – fibrous specimens at 28 days 40

Figure 4.9. SEM images a) PC TW NF-surface, b) PC SW NF-surface 41

Figure 4.10. EDAX microanalysis for the PC TW NF 42

Figure 4.11. EDAX microanalysis for the PC SW NF 43

Figure 4.12. SEM images a) SRC TW NF-surface, b) SRC SW NF-surface . . . 44

Figure 4.13. EDAX microanalysis for the SRC TW NF 45

Figure 4.14. EDAX microanalysis for the SRC SW NF 46

Figure 4.15. SEM images a) PC TW F, b) PC SW F 47

Figure 4.16. SEM images a) SRC TW F, b) SRC SW F 48

Figure 4.17. XRD results of center of the PC SW NF and PC TW NF specimens (F: Friedel's salt, Q: Quartz (SiO_2), E: Ettringite, CH: Portlandite ($Ca(OH)_2$), CSH: Calcium silicate hydrate, C: Calcite ($CaCO_3$), Albite ($NaAlSi_3O_8$), Clinochlore ((Mg,Fe)6(Si,Al)4O10$(OH)_8$)) . . 49

Figure 4.18. XRD results of surface of the PC SW NF and PC TW NF specimens (F: Friedel's salt, Q: Quartz , S: Calcium sulfate ($CaSO_4$), E: Ettringite, CH: Portlandite, CSH: Calcium silicate hydrate, C: Calcite, Albite ($NaAlSi_3O_8$), Clinochlore ((Mg,Fe)6(Si,Al)4O10$(OH)_8$)) 50

Figure 4.19. XRD results of center of the SRC SW NF and SRC TW NF specimens (F: Friedel's salt, Q: Quartz, S: Calcium sulfate, E: Ettringite, CH: Portlandite , CSH: Calcium silicate hydrate, C: Calcite, Albite ($NaAlSi_3O_8$), Clinochlore ((Mg,Fe)6(Si,Al)4O10$(OH)_8$)) 51

Figure 4.20. XRD results of surface of the SRC SW NF and SRC TW NF specimens (F: Friedel's salt, Q: Quartz (SiO_2), S: Calcium sulfate ($CaSO_4$), E: Ettringite, CH: Portlandite ($Ca(OH)_2$), CSH: Calcium silicate hydrate, C: Calcite ($CaCO_3$), Albite ($NaAlSi_3O_8$), Clinochlore ((Mg,Fe)6(Si,Al)4O10$(OH)_8$)) 52

LIST OF TABLES

Table 3.1. Materials of concrete 16

Table 3.2. Chemical composition and physical properties of Portland cement (PC) and sulfate-resisting cement (SRC) 17

Table 3.3. Properties of superplasticizer 18

Table 3.4. Physical properties of aggregates 18

Table 3.5. Sieve analyses results of aggregates 19

Table 3.6. Chemical characterization of the two types of mixing water 21

Table 3.7. Physical characteristics of fibers 22

Table 3.8. Mix ingredients 23

Table 3.9. Number of specimens in this study 24

Table 4.1. Fresh concrete properties 32

Table 4.2. Toughness values of the non - fibrous specimens 37

Table 4.3. Toughness values of the fibrous specimens 38

1. INTRODUCTION

Based on the United Nations World Water Report 2017, it is said that two-thirds of the world are suffering from water shortages during certain periods of the year [1]. With respect to the studies and estimates, this distress is increasing year by year. Since concrete is largely used building material in the world, this sector is also among the sectors that use significant amounts of water.

To use fresh water productively, the usage of seawater in the concrete industry seems compulsory. However, the usage of seawater as the concrete mixture is restrained in almost all standards around the world due to high chloride that increases corrosion of reinforcing steel. Seawater has an average salinity of 3.5%, about 78% of it is sodium chloride (NaCl) [2]. The problem of steel corrosion is solved either by using seawater in non-reinforced concrete applications such as non-corrosive synthetic structural fibers or by using non-corrosive material such as fiber reinforced polymer (FRP). This technique both increases the performance of concrete and shortens the material transportation process and brings down the cost and CO_2 emissions from construction work by efficient use of seawater when producing concrete in an area where fresh water is not readily available such as islands [3].

2. LITERATURE REVIEW

The rapid growth of the world's population can have significant impacts on resources in the world. For instance, fresh water will be famine and may be very difficult to obtain in some parts of the world.

In the concrete industry, several billion tons of fresh water is used annually in the mixing, curing, and cleaning in the world. Possibilities for the use of seawater as the mixing water in concrete should be seriously investigated to save fresh water [3].

When the researches are examined, it is understood that the use of seawater instead of the fresh water in the concrete is a topic that has been brought to the agenda many years ago, yet the subject is not very focused and a limited number of studies have been done [3].

As a result of a literature survey conducted by Nishida *et al.* [3], they give the number of published articles on the use of seawater as mixing water in concrete from 1974 to 2013. In recent years, interest in the subject has increased with the effect of decreasing water resources and climate change researches (Figure 2.1).

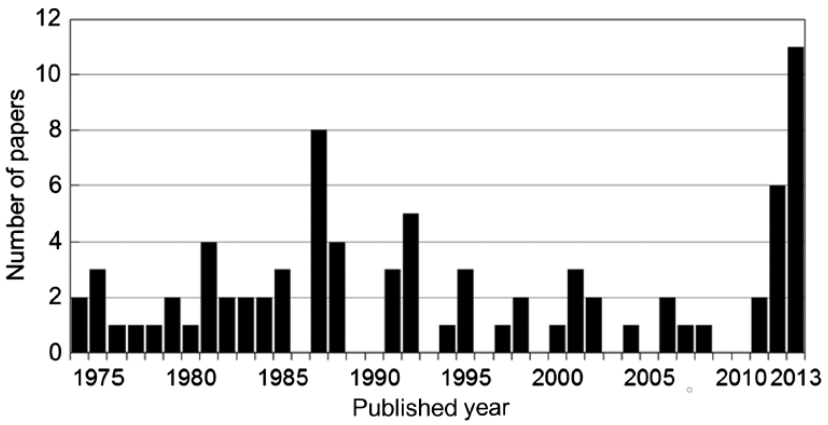

Figure 2.1. Number of articles published from 1974 to 2013 on the use of seawater as the mixing water in concrete [3]

2.1. Effects of Seawater as Mixing Water in Concrete

Mohammed *et al.* [4] have investigated concretes for 20 years under tidal environment. They found that the early strength of the concrete produced by seawater was better than tap water. According to the studies, the acceleration of hydration reactions with the effect of chloride in the seawater provided early improvement. On the other hand, after a prolonged exposure, there is no important difference between two types of concrete in terms of compressive strength.

Wegian [5] used seawater in the concrete for mixing and curing purposes and investigated its effects on mechanical properties. He also examined the effects of cement and aggregate used in the concrete in early and long-term ages, by testing tensile and bending strengths. As a result of this study, it was found that the resistance was high in the samples cast using seawater as the mixing water and cured in the seawater at early ages (7th day and 14th day), but the strength decreased in older ages (28th day and 90th day). Strength reduction increased with increasing exposure time, this may be due to salt crystallization formation which affects the strength gain. In addition, cement content had a significant effect on concrete strength and durability. For instance, higher cement content produced strength five times higher. Besides, using Sulfate Resisting Cement in the concrete improved the resistance of concrete against seawater and saline solutions. In this study, the long-term performance of concrete has not been investigated.

2.2. Effect of Mineral Additives on Concretes Produced by using Seawater as the Mix Water

Effects of mineral admixtures in concrete produced by using seawater has been tested by different researchers and positive results have been reported.

Katano *et al.* [6] used seawater and unwashed sea sand in the concrete. They have tried different combinations of fly ash, slag and silica fume with Portland cement as a binder material. They stated that the compressive strength, especially at an early

age, of the concrete produced by using seawater is higher than the strength of the concrete produced by tap water. They reported that increase in strength in 28 days varied between 3% and 70% according to the amount of the mineral additive. However, they stated that these increases were reduced to unimportant levels on the 90th days and ranged between 2% and 15%. These changes might be seen from Figure 2.2.

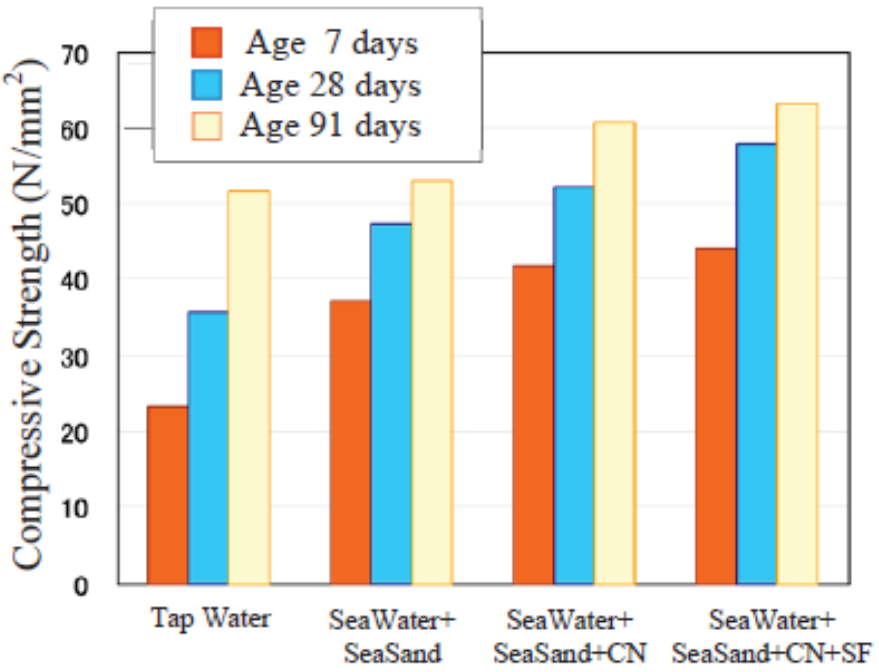

Figure 2.2. Compressive strength of concrete [6]

Otsuki *et al.* [7] used different binder materials such as Portland cement, Portland cement with fly ash and Portland cement with blast furnace slag and seawater in their study. The samples were exposed to seawater effect in the tidal region from 7 days to 20 years. In order to mathematically express the differences in compressive strength, they used the compressive strength ratio (concrete produced with seawater and concrete produced with tap water) and said that these ratios varied between 0.9 and 1.1 for all concretes. They stated that the type of mixing water had no serious effect on the compressive strength.

Bhaskar *et al.* [8] used ground granulated blast furnace slag (GGBFS) (40%, 50%, 60%) and fly ash (25%, 30%, 35%) with cement. They reported that they obtained

higher mechanical strengths (up to 28 days) for all fly ash mixtures and some slag mixtures in concretes with sea water. Results may be seen in Figure 2.3.

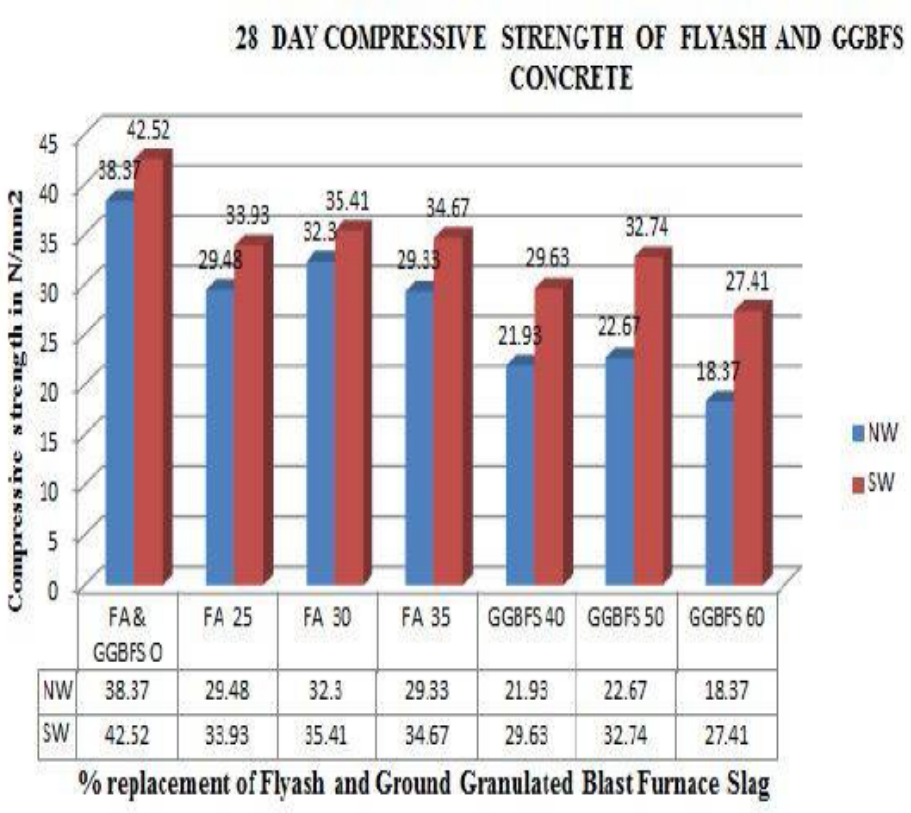

Figure 2.3. 28th day compressive strength with replacement fly ash and GGBFS in normal water (NW) and seawater (SW) [8]

In addition to compressive strength, Bhaskar *et al.* [8] also tested the tensile strength of the samples. 28th - day tensile strength of both fly ash mixtures and slag mixtures in concrete was less than the conventional mixture. According to authors, this decrease in strength owing to the replacement of cement with fly ash and slag can be attributed to the decrease in initial hydration. Moreover, the tensile strength of specimens cast by using the mix with fly ash replacement was reported to be more than the tensile strength of the specimens made by using GGBFS replacement. They also found that concretes made by using sea water yielded higher strength when compared to the concrete cast by using tap water. Results might be seen in Figure 2.4.

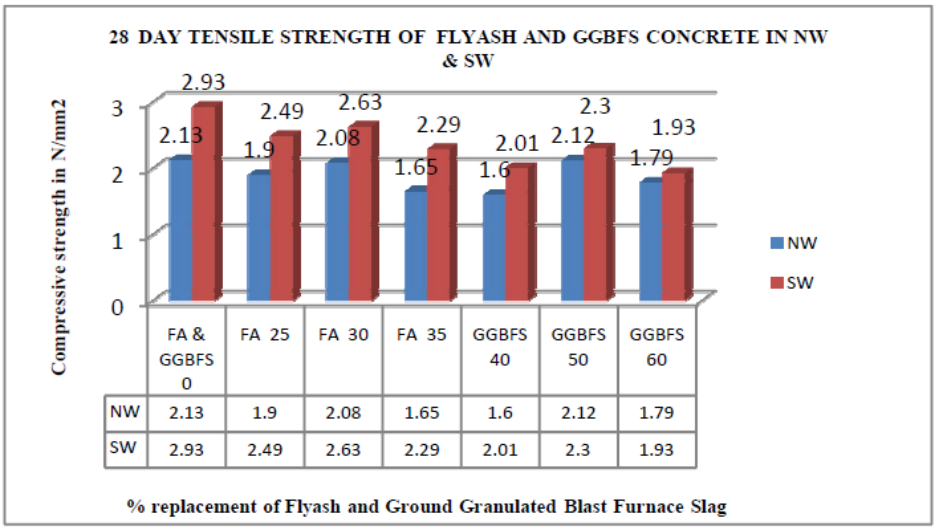

Figure 2.4. 28th - day tensile strength with replacement fly ash and GGBFS in normal water (NW) and seawater (SW) [8]

Shi *et al.* [9] used a small amount of metakaolin (0-6 %) as the mineral admixture and artificial seawater as the mixing water. They observed that the increase in the compressive strength of the concretes used in artificial seawater was higher than the use of tap water. The reason was that seawater accelerated the hydration of cement to increase the content of calcium hydroxide (CH) for pozzolanic reaction with metakaolin, which resulted in more calcium silicate hydrate (CSH) formed in the concrete.

Li *et al.* [10] have used metakaolin and seawater in the concrete. They reported that 56th-day compressive strength increased in using seawater as the mixing water in the concrete. They found that early strength (3rd and 7th days) increased significantly in seawater concretes. In the following days, they stated that the rate of increase was decreased because of the reaction of chloride ions with cement and metakaolin.

In all studies summarized above, it had been stated that the use of mineral additives in the concretes produced by seawater positively affected the mechanical strengths. Nishida *et al.* [3] also studied articles on "concrete produced with seawater". They reviewed numerous articles and stated that the use of slag or similar mineral additives and seawater in the concretes gave positive results.

2.3. Durability

In most of the studies related to the seawater as mixing water, early strength and 28-day strengths were only examined. It is obvious that the durability of the concrete produced by using seawater is very important. Few studies have been found on this subject.

The long-term studies (20 years) of Mohammed *et al.* [4] and Otsuki *et al.* [7] found that the strengths of the concrete produced by seawater were similar to that of fresh water. It was an important result. However, the durability of concrete produced by seawater could be examined in terms of shrinkage, resistance to sulfate attacks and freeze-thaw resistance.

It was thought that sulfate attack to concrete was caused by the reaction of magnesium sulfate ($MgSO_4$) and potassium sulfate with calcium hydroxide. Researches showed that magnesium sulfate attack was the most severe effect. Magnesium sulfate and calcium hydroxide ($Ca(OH)_2$, or CH) reaction resulted in soluble magnesium hydroxide and gypsum ($CaSO_4.2H_2O$). Ettringite formation ($3CaO.Al_2O_3.3CaSO_4.32H_2O$) was the result of the reaction of gypsum with C_3A and other aluminate hydration products. Şahmaran [11] reported that there were two mechanisms of ettringite formation of the damage occurring in the concrete: i) the pressure during the formation of ettringite crystals, ii) swelling of ettringite by water absorption. As the other results of the sulfate attack, it was stated that thaumasite formation ($CaCO_3.CaSO_4.CaSiO_3.15H_2O$) and calcium silicate hydrate gel ($3CaO.2SiO_2.3H_2O$, or C-S-H) might occur. The most effective method for reducing the sulfate damage was to limit the amount of C_3A in the cement content. In addition, it was stated that using cement with a low ratio of C_3S / C_2S reduced the amount of CH product, gypsum, and ettringite formation [11]. However, by reducing the amount of C_3A, it was stated that chloride binding would be reduced in the concrete containing chloride.

Another method of reducing sulfate damage was the use of mineral additives. Since the mineral additives reacted with CH and so that the amount of CH decreased.

Thus, the amount of CH that can react with sulfates was restricted [11].

Both Shi *et al.* [9] and Li *et al.* [10] reported that the use of seawater caused an increase the amount of CH at an early age, but the amount of CH in the microstructure decreased with the use of metakaolin. They also showed that chloride resistance increased with the use of metakaolin.

Wegian [5] focused on the effect of sulfate when assessing the damage to the concrete matrix produced by using seawater. According to the ACI Building Code 318-83, sulfate attack in concrete was classified as severe, when the sulfate ion concentration was higher than 1500 mg/l. In this case, the use of ASTM Type II cement and maximum water / cement ratio is allowed to exceed 0.5 were permitted in the normal concrete.

Katano *et al.* [6] found that the permeability of concrete produced by seawater decreased comparing to that of tap water due to the improvement of the microstructure. They reported that the freeze-thaw resistance could be achieved by entrained air of about 3.5% as in the normal concrete. They stated that the drying shrinkage of the concrete produced by seawater was lower than the drying shrinkage of the concrete produced by tap water.

2.4. Using Synthetic Structural Fibers in Concrete

Polymers are classified into 2 groups as natural polymers and synthetic polymers. Non-structural polymer-based fibers in concrete have been used for many years to prevent shrinkage cracks. These fibers can be may yield different properties.

Fallah and Nematzadeh [12] used macro - polymeric fibers (MP) (l = 39mm , l / d: 50) in different amounts (0.25% - 0.50% - 0.75% - 1.0% - 1.25%) and polypropylene fibers (PP) (l=12 mm, l/d: 631) in different amounts (0.1% - 0.2% - 0.3% - 0.4%- 0.5%) in their study. They reported that the modulus of elasticity and splitting tensile strength produced with macro - polymeric fibers increased with increasing amount of

fibers (Figure 2.5 and Figure 2.6).

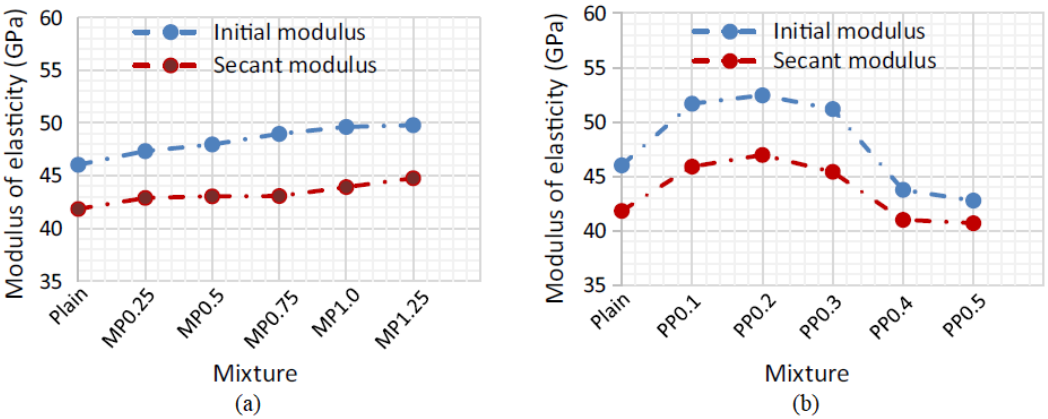

Figure 2.5. Modulus of elasticity for a) macro - polymeric fiber-reinforced concrete, b) polypropylene fiber-reinforced concrete [12]

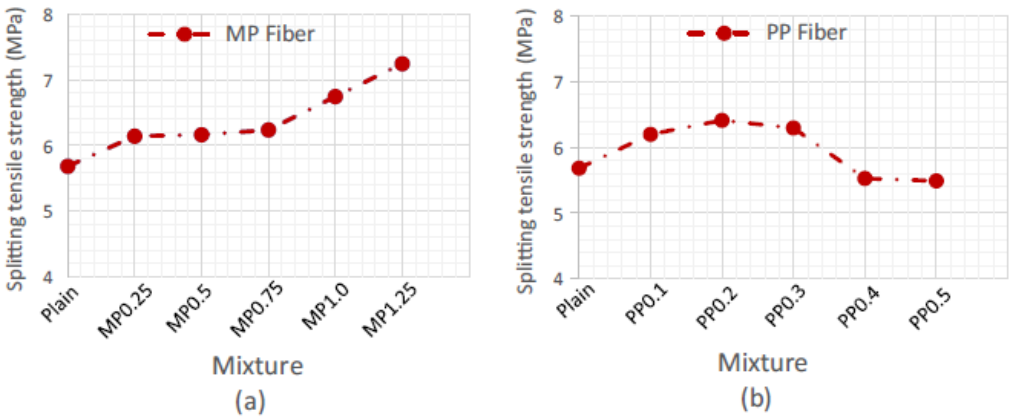

Figure 2.6. Splitting tensile strength for: a) macro - polymeric fiber-reinforced concrete, b) polypropylene fiber-reinforced concrete [12]

Hasan-Nattaj and Nematzadeh [13] produced two types of concrete with different amounts (0.2%, 0.35%, 0.5%, 0.65% and 0.8%) of micro-synthetic polymer fibers (1: 54mm, l / d: 159) and different amounts (0.5%, 0.75%, 1%, 1.25%, and 1.5%) of hooked -end steel fibers (l:50 mm, l / d: 62.5). When compared micro-synthetic polymer fiber-reinforced concrete and steel-fiber concrete, they found that the loss of workability in the concretes produced with synthetic fibers was higher than that of steel fibers. They stated that better results of the splitting tensile strengths were obtained when steel

fibers were used in the concrete. They also reported that the synthetic fibers provided much more improvement of the modulus of elasticity of the concrete, and they also measured lower void ratio and water absorption in the synthetic fiber concretes.

2.5. Differences of the Microstructure

Katano *et al.* [6] said that, according to SEM images, many needle crystals of ettringite were formed in the pores of concrete mixed using seawater and these crystals filling large voids densified the microstructure. It can be seen in Figure 2.7. In addition, in terms of XRD results, Figure 2.8 showed that the ettringite formation in concrete using seawater was approximately 30% greater than in concrete using tap water. The increase in ettringite formation was found to be approximately 120% with sea water and special admixture which was containing calcium nitrate (CN).

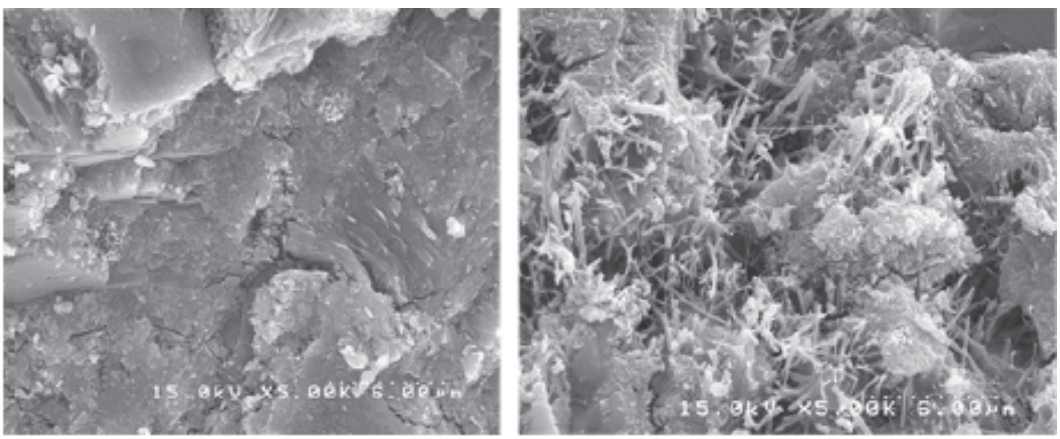

Figure 2.7. SEM images of mortars for: a) tap water + CN + silica fume (SF), b) seawater + CN + silica fume (SF) [6]

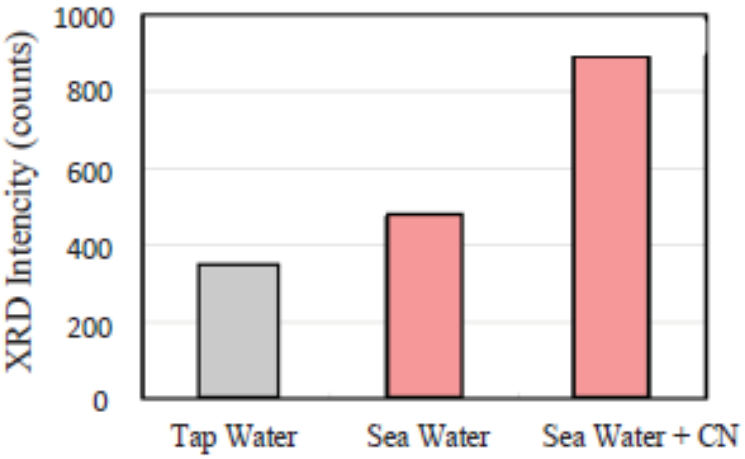

Figure 2.8. XRD intensity of ettringite in the concrete [6]

Etxeberria *et al.* [14] used two types of aggregate, recycled aggregates of mixed composition (MRA) and recycled aggregate concretes (RAC), Portland cement, cement incorporating blast-furnace slag (BFS), fresh water and seawater. According to XRD analysis of concretes produced by using seawater and sulfate resistant cement (CEM I 42.5 R) and blast furnace slag cement (CEM III 42.5), accumulation of the ettringite and the ingress of chlorides can produce the larger size of solid phase Friedel's salt in the pores.

Federica *et al.* [15] used seawater, fresh water, salt-contaminated aggregates, fly ash and a combination of innovative cement to produce different concrete mixtures. Mineral phase amounts of cement pastes were determined during the hydration process by XRD-Rietveld analysis. The hydration of the reference cement with tap water has included a very high amount of portlandite formation and ettringite from the beginning; a large amount of amorphous phase was detected. However, the amount of ettringite of innovative cement (Seacon cement) with fresh water was higher than in the previous case, while a reduced content of portlandite was measured. The use of seawater, the presence of carbonates and chloride ions, causes the formation of AFm phases, hemicarbonate and calcium-chloroaluminate phases (known as Friedel's salt).

According to the aforementioned report by Shi *et al.* [9], more Friedel's salt was observed in the concrete produced by using metakaolin and seawater when XRD analysis was performed. Figure 2.9 showed that metakaolin promoted the formation of Friedel's salt under the condition of seawater mixing. They stated that this salt was formed as a result of C_3A and $CaCl_2$ reaction. After the Friedel's salt was formed, chloride ions were bound to the concrete, and so that chloride resistance increased with the metakaolin. In addition, they reported that the negative effects of using seawater could be eliminated by the usage of metakaolin.

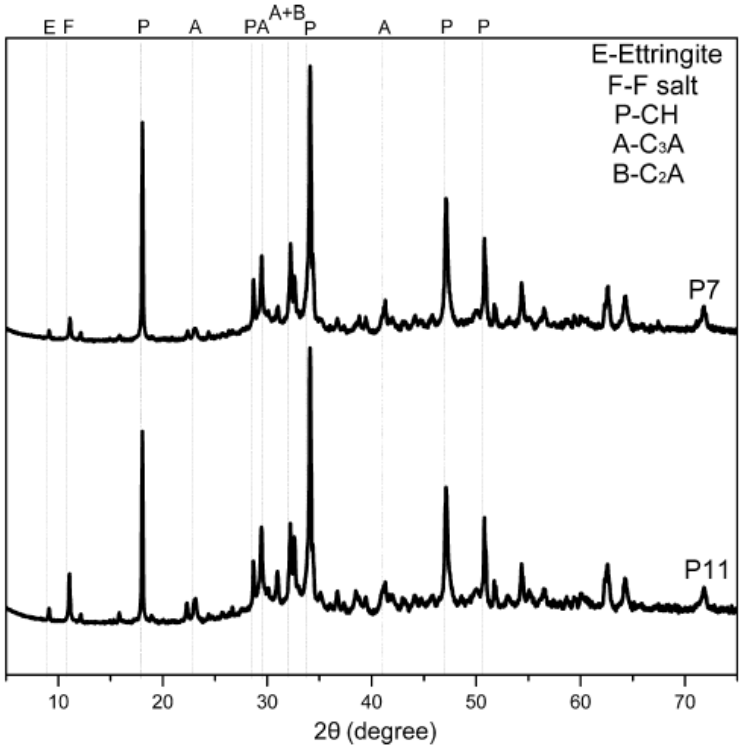

Figure 2.9. XRD result of the non-MK + seawater mix (P7) and MK+seawater mix (P11) [9]

Mohammed *et al.* [4] reported the strengths of two separate sections. Series 1 and Series 2 exposured to the tidal environment up to 15 years and 20 years, respectively. They stated that using seawater (Series 1) caused an earlier strength gain comparing to the same mixture with fresh water. It was expected owing to the acceleration of the hydration process with the presence of chloride. In addition, according to XRD analyses, Friedel's salt (mostly on the sample surfaces) and calcium carbonate (gen-

erated from the reaction of calcium hydroxide (CH) with dissolved CO_2 in seawater) were observed in all samples of Series 2.

2.6. Effects of Seawater on Shrinkage Strain of Concrete

Katano *et al.* [6] said that, the autogenous shrinkage strain of concrete mixed with seawater was slightly larger than that of fresh water. Contrary to this, the drying shrinkage strain of the concrete mixed using seawater was smaller than that of the concrete with tap water and it may be seen in Figure 2.10.

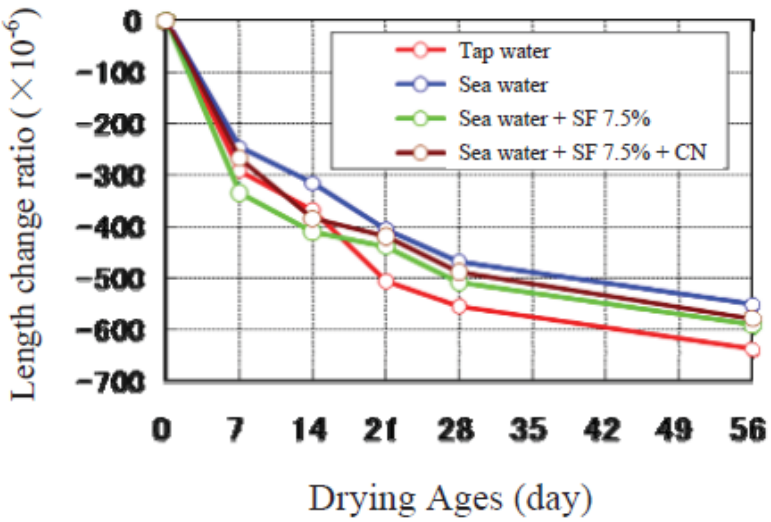

Figure 2.10. Length change ratio owing to drying shrinkage [6]

Etxeberria *et al.* [14] used both recycled aggregates of mixed composition (MRA) and recycled aggregate concretes (RAC) and mixed using Portland cement, cement incorporating blast-furnace slag (BFS), fresh water and seawater. They reported that when concretes were produced with recycled aggregates and seawater, plastic shrinkage was lower and concretes produced with BFS cement employing recycled aggregates accomplished minimum plastic shrinkage.

Federica *et al.* [15] examined 4 different mixtures that were produced using seawater, fresh water, salt-contaminated aggregates, fly ash and a combination of innovative

cement. They reported that the addition of high chloride content ingredients (SEA-CON cement, seawater, and recycled concrete aggregates) had negative effects causing increased shrinkage. It might be shown in Figure 2.11.

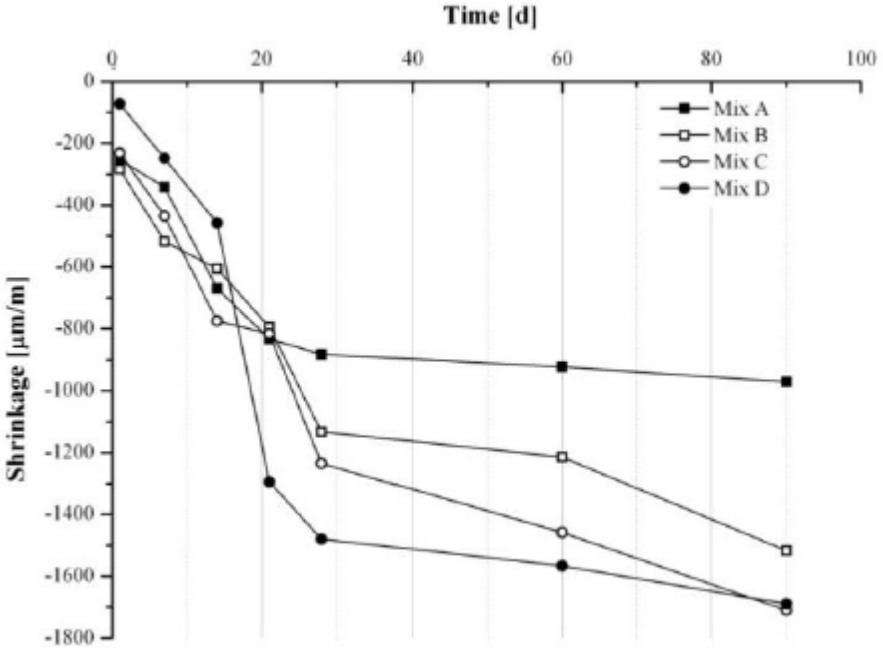

Figure 2.11. Drying shrinkage of concretes (Mix A : Reference cement+fly ash+fresh water, Mix B: Seacon cement+ fly ash+fresh water, Mix C: Reference cement+fly ash+seawater, Mix D: Reference cement+fly ash+fresh water+RCA) [15]

Younis *et al.* [2] produced two types of concrete mixtures. Mix A was produced with the use of fresh water, represented the reference mixture. Mix B was produced with the use of seawater. Shrinkage tests were performed in accordance with ASTM C157/C157M. They reported that Mix B had highest drying shrinkage due to the presence of chloride in the pore solution (Figure 2.12).

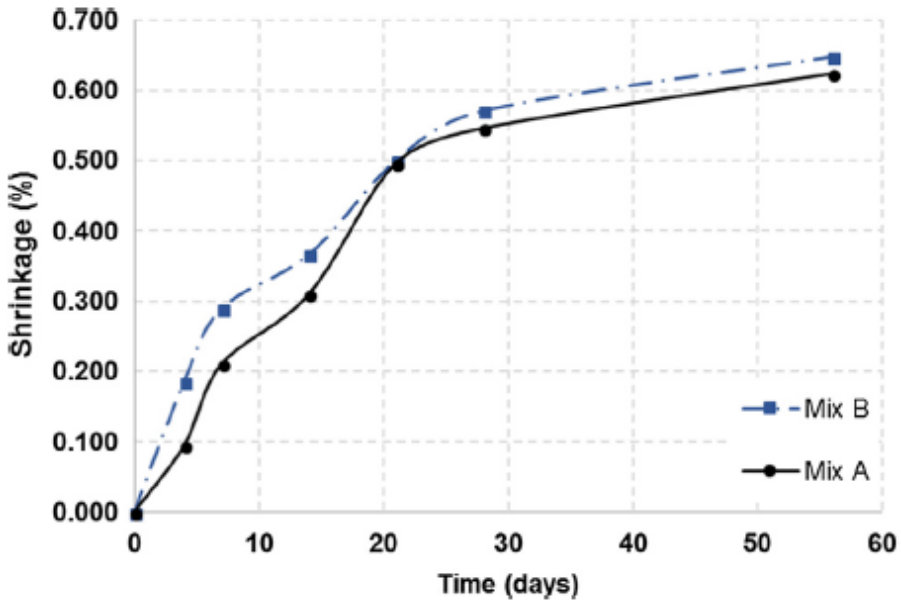

Figure 2.12. Shrinkage test results [2]

3. EXPERIMENTAL STUDY

3.1. Materials

Table 3.1 gives the materials of concrete used for the tests. Tap water or seawater was used for mixing. Portland cement or sulfate-resisting cement was used as binding material. A chemical admixture was used as a superplasticizer.

Table 3.1. Materials of concrete

Material	Description	Code	Specification
Water	Tap Water	TW	Cl^-: 39.78 mg/L
	Sea Water	SW	Cl^-: 10068 mg/L
Binder	Portland Cement	PC	Density: 3,14 g/cm^3
	Sulfate-Resisting Cement	SRC	Density: 3,06 g/cm^3
Fine Aggregate	Crushed Sand	CS	Density: 2,7 g/cm^3
	Natural Sand	NS	Density: 2,63 g/cm^3
Coarse Aggregate	Coarse Aggregate- No 2	No 2	Density: 2,72 g/cm^3
	Coarse Aggregate- No 1	No 1	Density: 2,72 g/cm^3
Fiber	Structural Macro Synthetic	F	Density: 0,91 g/cm^3
Admixture	Superplasticizer	SP	Density: 1,08 g/cm^3

3.1.1. Cement

In this study, Ordinary Portland cement (CEM I 42.5R) and sulfate-resisting cement (SRC) were used as binding materials. Physical, chemical properties and strength characteristics of the types of cements were given in Table 3.2 and Table 3.3.

Table 3.2. Chemical composition and physical properties of Portland cement (PC) and sulfate-resisting cement (SRC)

	PC	**SRC**
Al_2O_3 (%)	5.58	6.7
Fe_2O_3 (%)	3.32	4.45
CaO (%)	63.67	53.97
MgO (%)	1.25	1.61
Na_2O (%)	0.21	0.57
K_2O (%)	0.68	0.85
SiO_2 (%)	19.63	26.15
SO_3 (%)	3.23	2.56
Cl (%)	0.0423	0.0305
Loss on ignition (%)	2.03	2.28
Insoluble residue (%)	0.28	13.31
Free CaO (%)	2	1.11
Le Chatelier (mm)	1	1
Specific gravity (kg/m^3)	3140	3060
Residue on 45 μm sieve (%)	4.5	3.3
Residue on 90 μm sieve (%)	0.0	0.2
Residue on 200 μm sieve (%)	0.0	0.0
Blaine specific surface (cm^2/gr)	3607	4092
Initial setting time (min)	100	147
Final setting time (min)	165	221
C_3S	50.36	-
C_2S	18.37	-
C_3A	9.18	-
C_4AF	10.10	-
2 days (MPa)	28.3	24.9
28 days (MPa)	54.8	54.4

3.1.2. Admixtures

In this study, a polycarboxylic ether based admixture was used as the superplasticizer. It was utilized in the mixes in order to maintain a slump of about 19±2 cm. Properties of superplasticizer can be showed in Table 3.3.

Table 3.3. Properties of superplasticizer

Aspect	Light brown liquid
State	Liquid
Relative Density	1080 ± 10 at 25 °C
pH	≥6
Chloride ion content	0.2%

3.1.3. Aggregates

Four types of aggregates which were crushed sand, natural sand and two coarse aggregates of different sizes were used in this study. To determine the gradation or the distribution of aggregate particles by size, sieve analysis was performed.

Table 3.4. Physical properties of aggregates

Aggregates	Density (g/cm^3)
No 1	2.72
No 2	2.72
Natural Sand	2.63
Crushed Sand	2.70

3.1.3.1. Sieve Analysis of Aggregates. Sieve analyses of coarse aggregates were done according to TS 802 [16]. In this study, maximum aggregate size (D_{max}) was 25 mm. The volumetric amounts for natural sand, crushed sand, No 1 and No 2 were determined as 15%, 35%, 30%, and 20%, respectively. Sieve analysis results of aggregates were given in Table 3.5. Gradation curve of the mixture was also shown in Figure 3.1.

Table 3.5. Sieve analyses results of aggregates

Sieve Size(mm)	NS(passing%)	CS(passing%)	No 1(passing%)	No 2(passing%)
31.5	100	100	100	100
25	100	100	100	99.51
16	100	100	100	35.52
12.5	100	100	98	6.9
8	100	100	66.65	0.84
4	99.62	99.62	5.84	0.44
2	95.04	95.04	1.24	0.4
1	81.98	81.98	1.09	0.38
0.5	67.19	67.19	1.05	0.34
0.25	9.75	9.75	0.94	0.29
0.125	1.68	1.68	0.54	0.19
0.074	0.59	0.59	0.4	0.14

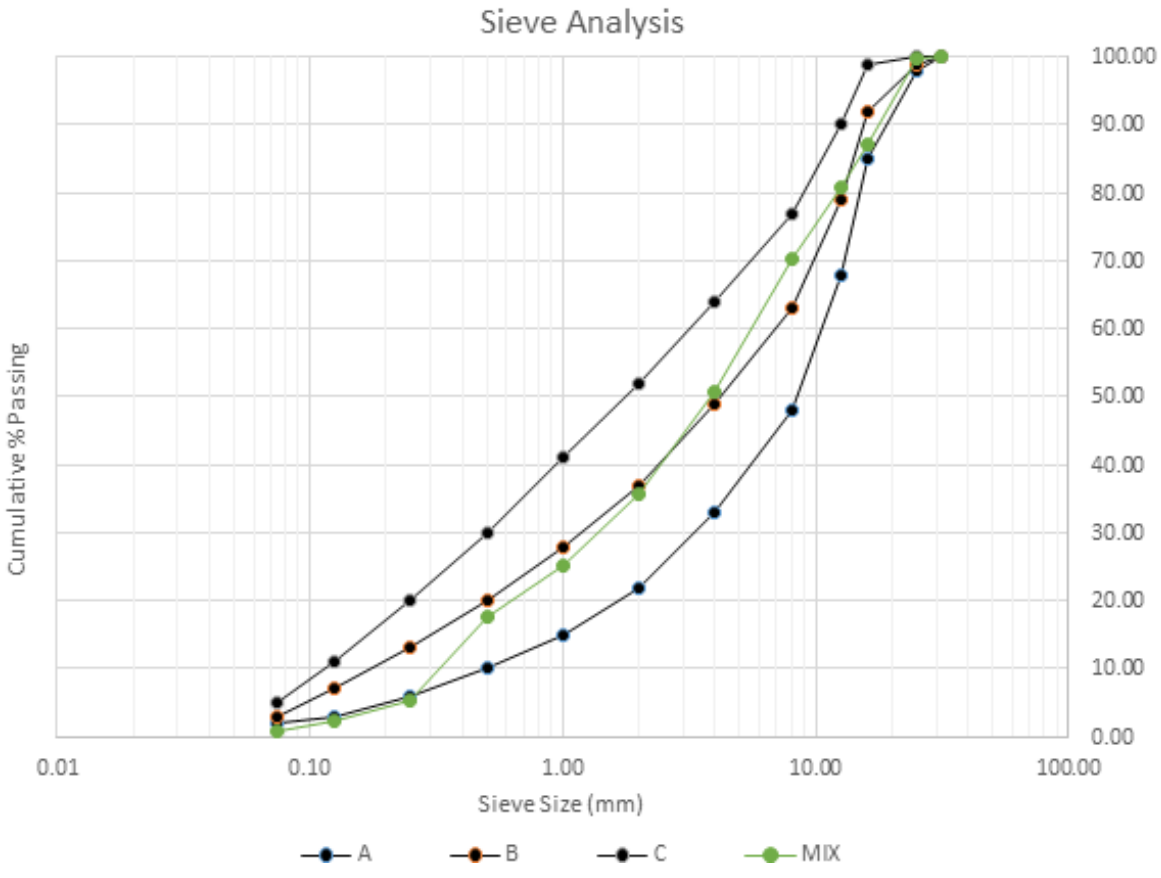

Figure 3.1. Gradation curve of the mixture

3.1.4. Water

In this study, two types of mixing water which were seawater and tap water were used. The seawater was brought from the Black Sea in Sarıyer, Istanbul.

Chemical characterization was performed for both types of mixing waters, including the determination of chlorides, sulfates, magnesium, calciums, potassiums, sodiums and pH (at 21 °C). Chemical characterization results for both water types as per the corresponding methods/standards were given in Table 3.6.

Table 3.6. Chemical characterization of the two types of mixing water

	Results		Standard	
	Tap Water	Seawater	Tap Water	Seawater
Sodium (Na), mg/L	24.3	4420	SM 3111 B	SM 3111 B
Potassium (K), mg/L	3.92	193	SM 3111 B	SM 3111 B
Calcium (Ca), mg/L	51.85	234	TS 6228 [17]	TS 6228 [17]
Magnesium (Mg), mg/L	8.18	638	TS 6228 [17]	TS 6228 [17]
Chloride (Cl^-), mg/L	39.78	10068	SM 4110 [18]	TS 4164 [19]
Sulfate (SO_4^{2-}), mg/L	76.97	1178	SM 4110 [18]	TS 5095 [20]
Organic Substance	Normal	Normal	TS 1008 [21]	TS 1008 [21]
pH	7.06	8.61	TS 10523 [22]	TS 10523 [22]

3.1.5. Fiber

For this study, structural macro synthetic fibers were selected and used in the mix. Physical characteristics of fibers were given in Table 3.7. An image of structural macro synthetic fibers was also shown in Figure 3.2.

Table 3.7. Physical characteristics of fibers

Raw material	Polypropylene
Specific gravity	0.91
Length (mm)	40
Diameter (mm)	0.72
Tensile stress (MPa)	550
Alkali resistance	Excellent
Resistance to corrosion	Excellent
Melting temperature (°C)	160
Resistance to corrosion	Excellent
Number of fibers/kg	50000

Figure 3.2. Structural macro - synthetic fibers

3.2. Mix Proportions

In this study, concrete mixes were cast by using two different cement types, Ordinary Portland cement, and Sulfate Resistant cement, and both fibrous (0.5% vol.) and non-fibrous samples were produced. Seawater and tap water were used as the mixing water for concrete. It was aimed to have a concrete complying a strength class of C40/50. Water-to-cement ratio was taken to be 0.45. A polycarboxylic ether based admixture was used in all mix types in order to maintain approximately the same slump value of 19±2 cm.

For all mixes, the same procedure was used. After weighing of materials, first, dry ingredients were put into the pan and mixed for two minutes. After that mix water containing all of the superplasticizers was added to the mix in two minutes and the materials were stirred for another two minutes to obtain a homogenous concrete. All the mix proportions were shown in Table 3.8.

Table 3.8. Mix ingredients

Sample Code	C	W	NS	CS	No 1	No 2	SP	F
PC-TW-NF	410	184	280	661	563	378	2.91	-
PC-TW-F	410	184	280	661	563	378	3.88	4.5
PC-SW-NF	410	184	280	661	563	378	2.91	-
PC-SW-F	410	184	280	661	563	378	3.47	4.5
SRC-TW-NF	410	184	280	661	563	378	5.37	-
SRC-TW-F	410	184	280	661	563	378	5.41	4.5
SRC-SW-NF	410	184	280	661	563	378	5.41	-
SRC-SW-F	410	184	280	661	563	378	4.92	4.5

PC and SRC stand for Portland cement and sulfate resistant cement, respectively. TW and SW represent tap water and seawater, while F and NF show fibrous and non-fibrous specimens, respectively.

3.2.1. Specimen Curing

All specimens were cured in a curing tank as suggested by EN 12390-2 standard [23]. Specimens were removed from their molds after 1 day and kept in the curing tank until the test day. The temperature of curing water was set at around 20 ± 2 °C as suggested in EN 12390-2 standard.

3.2.2. Number of Specimens

Compressive strength tests were performed on 15x15x15 cm cube specimens. Modulus of elasticity tests were carried out on cylinder samples with 10 cm in diameter and 20 cm in height. In addition, three - point bending tests were performed on 10x10x50 cm beam samples and length change tests were carried out on 7.5x7.5x28.5 cm beam specimens. Microstructural analyses (ESEM and XRD) were performed by taking samples from certain regions after three - point bending testing on the beams. In total, 48 cube samples, 48 cylinder specimens and 44 different sizes of the beam samples were produced (Table 3.9).

Table 3.9. Number of specimens in this study

Sample Code	Compressive strength/ Modulus of elasticity (7 and 28 days)	Three - point bending test (28 days)	Length change test (28 days)
PC-TW-NF	6/6	3	5
PC-TW-F	6/6	3	-
PC-SW-NF	6/6	3	5
PC-SW-F	6/6	3	-
SRC-TW-NF	6/6	3	5
SRC-TW-F	6/6	3	-
SRC-SW-NF	6/6	3	5
SRC-SW-F	6/6	3	-

3.3. Experimental Methods

3.3.1. Fresh State Tests

After mixing of materials slump tests and density measurements were conducted on fresh concrete. Slump tests were performed according to TS EN 12350-2 standard [24].

3.3.2. Hardened State Tests

3.3.2.1. Compressive Strength Tests. Load controlled compressive strength tests were carried out on 15x15x15 cm cube specimens according to BS EN 12390-3 standard [25] at the ages of 7 and 28 days to observe strength evolution of the specimens. Specimens were axially loaded at a rate of 13.5 kN/s (0.6 MPa/s). The compressive strengths of the cube specimens were calculated by dividing the maximum load reached during the compressive strength test by the cross-sectional area of the specimens. For all of the 8 different series, three cube specimens were tested for average values.

3.3.2.2. Modulus of Elasticity Tests. Modulus of elasticity tests were performed on 10 x 20 cm cylindrical specimens according to BS EN 12390-13 / Method A (Determination of Initial and Stabilized Secant Modulus of Elasticity) [26]. Loading procedure of the mentioned method consists of eleven loading cycles and details of the cycles were given in Figure 3.3. Cylindrical specimens were loaded according to given loading procedure by using MTS servo - hydraulic test machine that has 500 kN of maximum loading capacity. During the loading procedure, rate of rising and fall set to 10.6 kN/sec for all cycles, and frame with two Linear Variable Differential Transformers (LVDTs) were attached to the cylindrical samples to measure the axial length changes in the specimens during the loading process. Modulus of elasticity test setup was given in Figure 3.4.

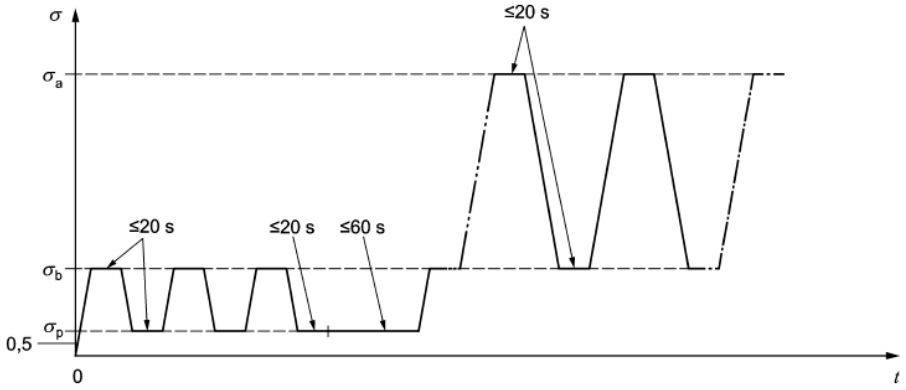

Figure 3.3. Loading procedure for the determination of initial and stabilized secant modulus of elasticity [27]

In Figure 3.3, is the applied stress in MPa, t is time in second, $(_a)$ is upper stress that is equal to 1/3 of the compressive strength (f_c) of the specimens, $(_b)$ is lower stress that is between 0,10 x (f_c) and 0,15 x (f_c) , $(_p)$ is preload stress that is between 0,5 MPa and b . It should be noted that preload stress was accepted 1 MPa.

In order to determine approximate compressive strength (f_c) of the modulus of elasticity specimens that is mentioned above, compression tests according to BS EN 12390-3 [25] were carried out on reference 15x15x15 cm cube specimens. Measured values were multiplied by 0,8 to find an approximate mean compressive strength for the cylindrical specimens.

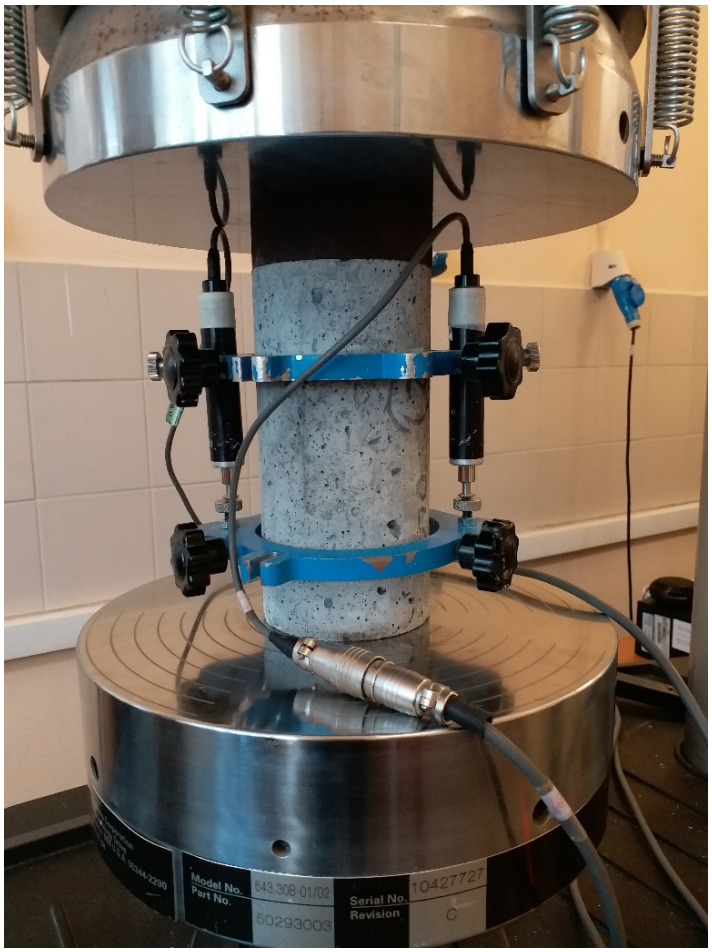

Figure 3.4. Modulus of elasticity test setup

3.3.2.3. Three - Point Bending Test. CMOD controlled three – point bending tests according to JCI-S-001 [27] and JCI-S-002 [28] were carried out for all beam specimens. The first standard was used for non-fibrous beams, latter was used for fibrous beams. Tests were performed on 3 prismatic 30 mm notched specimens that have 100 mm width and height and 500 mm length, by using the test setup given in Figure 3.6. When testing non-fibrous beams, CMOD increase rate was set to 0.1 mm/min and the test was continued until the fracture occurred. In addition, when testing fibrous beams, CMOD increase rate was set to 0.4 mm/min and the tests were continued until the CMOD value reached 3 mm. Furthermore, to measure midspan deflection of the specimens during the loading applications, 2 LVDTs were placed on both sides of the specimens, as seen in Figure 3.5.

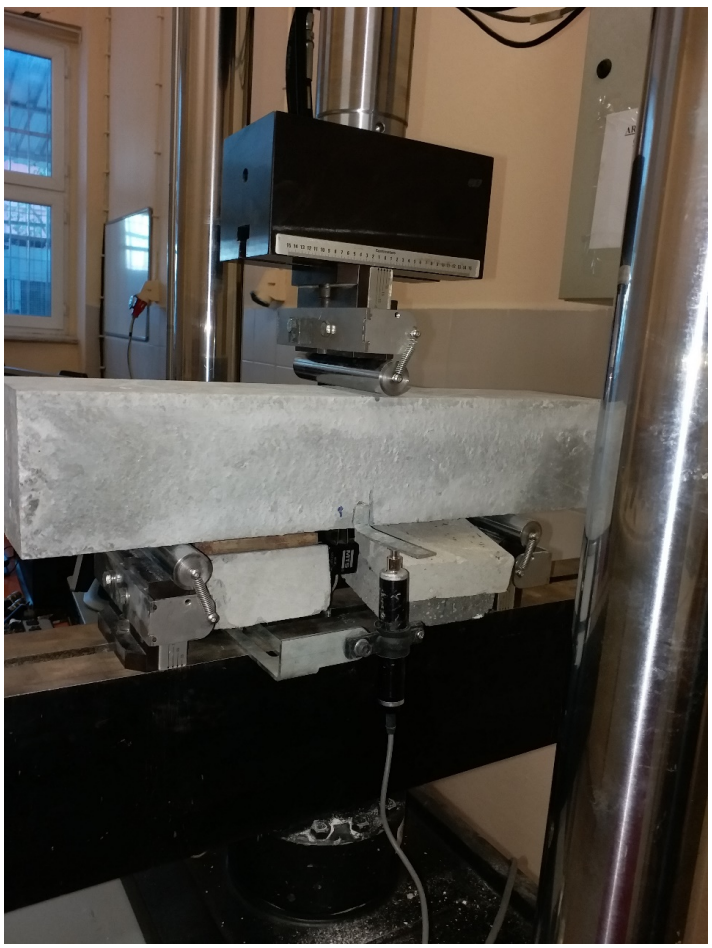

Figure 3.5. Three - point bending test setup

3.3.2.4. Length Change Tests. Length change tests according to ASTM C157 [29] were carried out on 7.5 x7.5x28.5 cm beam specimens. The molds were prepared for concrete casting. After 24 h, concrete prisms were demolded and immersed in water (23±2 °C) for 30 min, then initial length measurements (initial CRD) were taken. Concrete specimens were then stored in a curing pool and after 28 days the comparator readings (CRD) were repeated. Length change of specimens at 28 days was calculated as given in Equation 3.1 [29].

$$\Delta L_x(\%) = \frac{(CRD - initialCRD)}{G} x100 \tag{3.1}$$

ΔL_x= length change of specimen at any age, %

CRD= difference between the comparator reading of the specimen and the reference bar at any age

G= the gage length (250 mm)

3.3.2.5. Microstructural Analyses. After bending tests, samples were taken from the maximum moment region of the beams (near the crack) for microstructural investigations and the hydration products were examined. Samples were taken from both the surface and the center of the beams (Figure 3.6). For the SEM / EDAX observations, eight different mixtures were sampled. For the XRD analyses, only non-fibrous concrete samples were taken. Microstructural tests are very significant for explaining the strength or damage development in the concrete. These tests are also important to see the differences which may occur due to use of seawater/tap water and PC/SRC in this study.

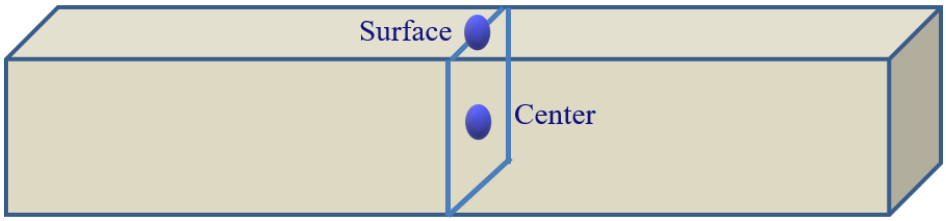

Figure 3.6. Sampling locations for SEM analysis

- SEM / EDAX Observations

A scanning electron microscope equipped with energy dispersive X-ray analysis (SEM/EDAX) was used to understand the morphological changes in concrete. All ESEM/EDAX analyses are conducted by FEI-Philips XL30 ESEM-FEG / EDAX system located in the Boğaziçi University Advanced Technologies Research and Development Center electron microscopy and microanalysis unit.

Specimens were taken from both the surface and the center of the beams and were prepared for the examination. Since concrete is not a conductive material, a thin gold-plating layer is applied to prevent blurred images after the bombardment of weak electrons into the sample. In addition, the accelerating voltage is kept constant and the value is 20 kV.

Figure 3.7. A test sample of fibrous-concrete for ESEM / EDAX analysis

- X - Ray Diffraction (XRD) Analyses

XRD analyses were performed on powder samples obtained from both the surface and center of the non-fibrous concrete beams. For the XRD analyses, four different non-fibrous concrete samples were taken. XRD analyses are conducted by A Rigaku D/MAX-Ultima+/PC X-ray diffraction equipment located in the Boğaziçi University Advanced Technologies Research and Development Center. Hydration products analyses in the non-fibrous concrete were determined by the XRD analyses.

4. RESULTS AND DISCUSSION

4.1. Fresh Concrete Properties

All of concrete mixes were cast to obtain a slump of 19±2 cm. Slump tests results and densities of fresh concrete are reported in Table 4.1.

Table 4.1. Fresh concrete properties

Sample Code	Slump (cm)	Density (kg/m^3)
PC-TW-NF	18	2441
PC-TW-F	19	2428
PC-SW-NF	17	2438
PC-SW-F	19	2427
SRC-TW-NF	21	2412
SRC-TW-F	21	2411
SRC-SW-NF	19	2423
SRC-SW-F	19	2410

As seen in Table 4.1, almost all mixes had similar slump values, ranging between 17-21 cm, and densities, ranging between 2410-2441 kg/m^3.

4.2. Hardened Concrete Properties

4.2.1. Compressive Strength Analysis

Load controlled compressive strength tests were performed on cube specimens at the ages of 7 and 28 days to observe strength evolution of the samples. Specimens were axially loaded at a rate of 13.5 kN/s (0.6 MPa/s) until failure. For all of the 8 different mixes, three cube samples were tested. Both non-fibrous and fibrous samples were compared. The values shown in Figure 4.1 and Figure 4.2 were average compressive

strengths of the three non-fibrous and fibrous cube samples, respectively. The standard deviations between the compressive strengths of the three samples were shown in the graphs.

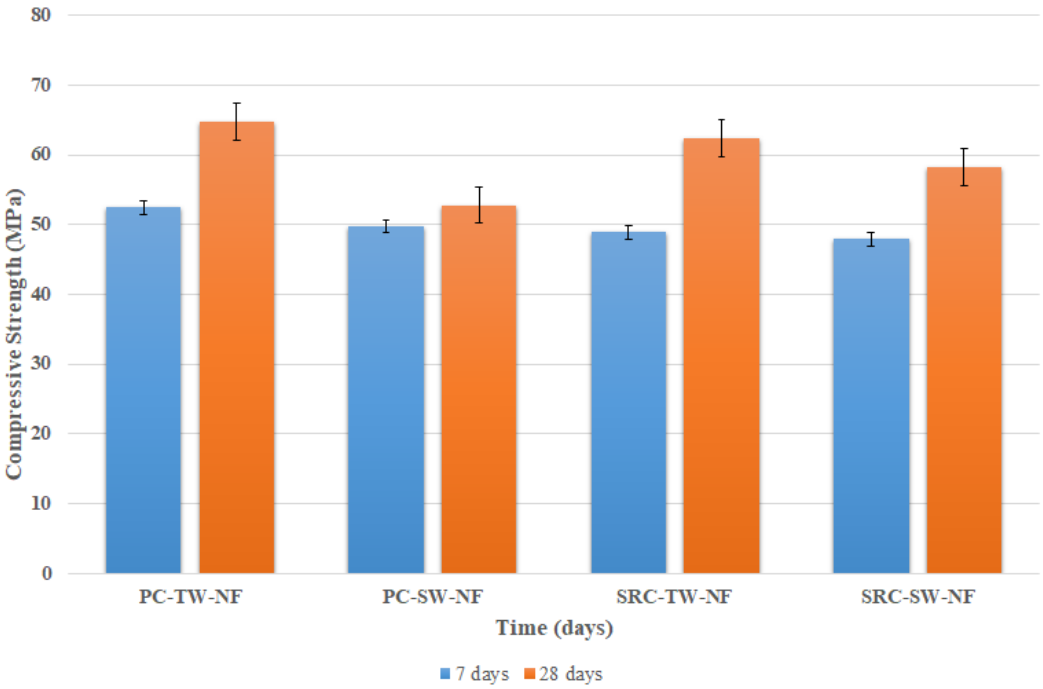

Figure 4.1. Compressive strength of non-fibrous specimens

Based on Figure 4.1, compressive strength was decreased when seawater was used in non – fibrous mixtures. However, no significant effect on compressive strength was seen when seawater was used in fibrous mix (Figure 4.2).

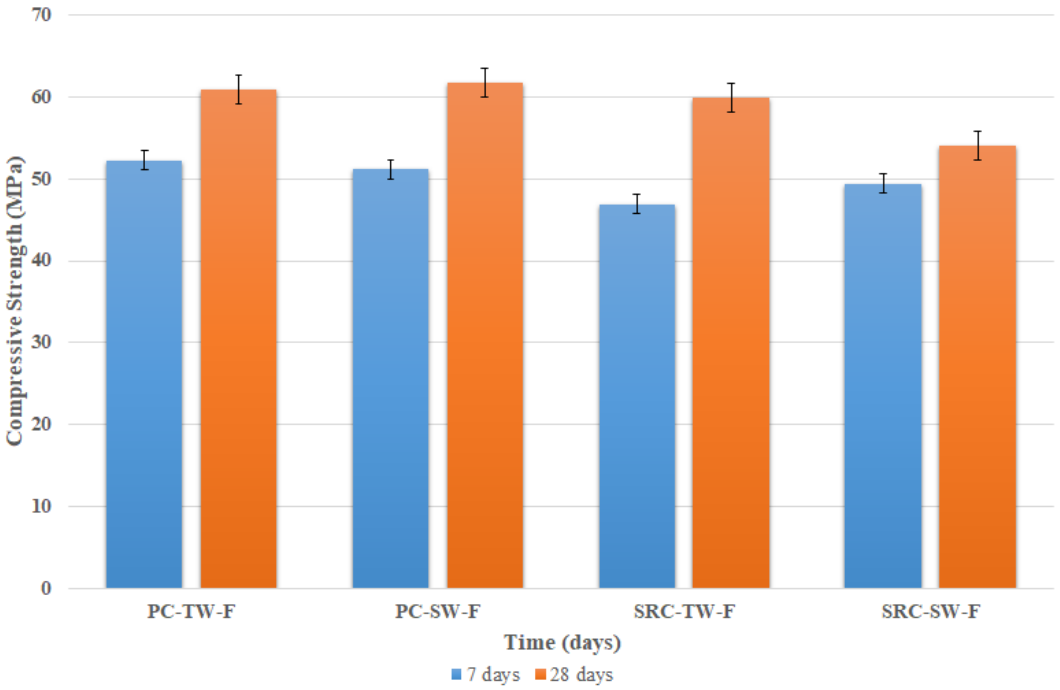

Figure 4.2. Compressive strength of fibrous specimens

When literature was reviewed, Federica *et al.* [15] reported that the use of seawater in the concrete decreased the long-term (90 days) compressive strengths. According to the experimental studies of Shi *et al.* [9], the compressive strength of concrete mixed with seawater was higher than that of the concrete mixed with fresh water at the same age. They reported that the combination of metakaolin and seawater improved the mechanical performance of concrete. Younis *et al.* [2] said that, using seawater resulted in a slight increase in the compressive strength of the concrete at early ages (3 and 7 days), but the long-term compressive strength of the concrete mixed with seawater (28 days) was 7–10% lower than that of fresh water. According to Mohammed *et al.* [4], the use of seawater caused an earlier strength gain compared to the same with tap water due to the acceleration of hydration process with the presence of chloride.

As can be understood from the results of this study and above summarized literature, different results may be obtained depending on the materials and mix design used. No negative effects of sea water was observed in this study for the 1st 28 days. However, different results can be obtained in the long term.

4.2.2. Modulus of Elasticity Test Results

Modulus of elasticity tests were performed on 4 types of fibrous and non-fibrous cylindrical specimens that were cured in 7 and 28 days. Tests were carried out according to BS EN 12390-13 / Method A (Determination of Initial and Stabilized Secant Modulus of Elasticity), and stabilized secant modulus of elasticity values were specified according to equation 4.1 [27].

$$E_{c,s} = \frac{\Delta\sigma}{\Delta\varepsilon s} = \frac{\sigma_a - \sigma_p}{\varepsilon_{a,3} - \varepsilon_{p,2}} \tag{4.1}$$

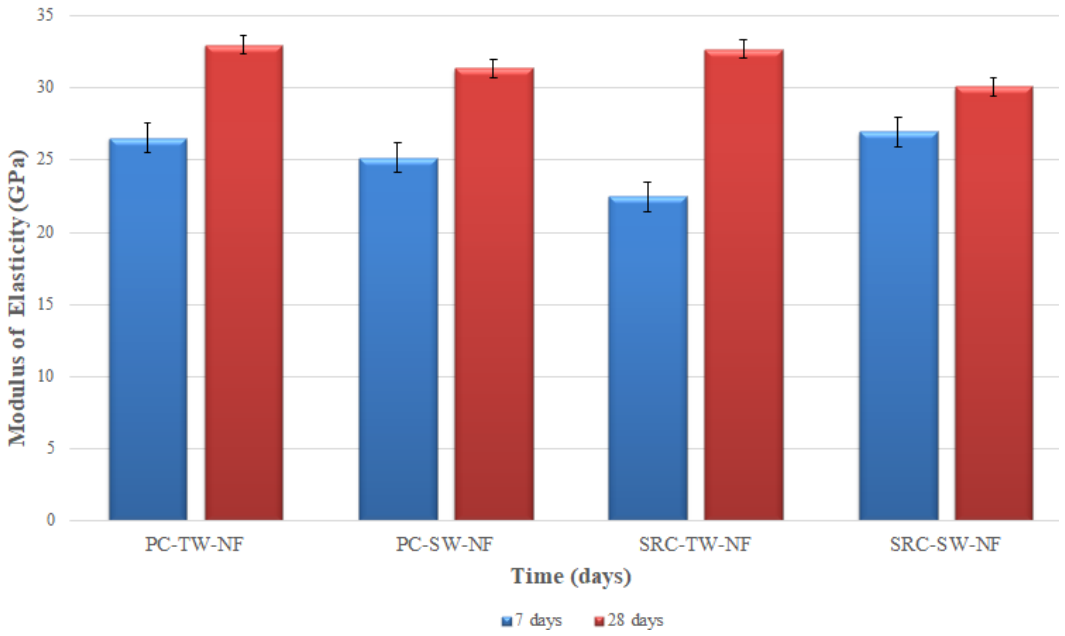

Figure 4.3. Modulus of elasticity of non - fibrous specimens

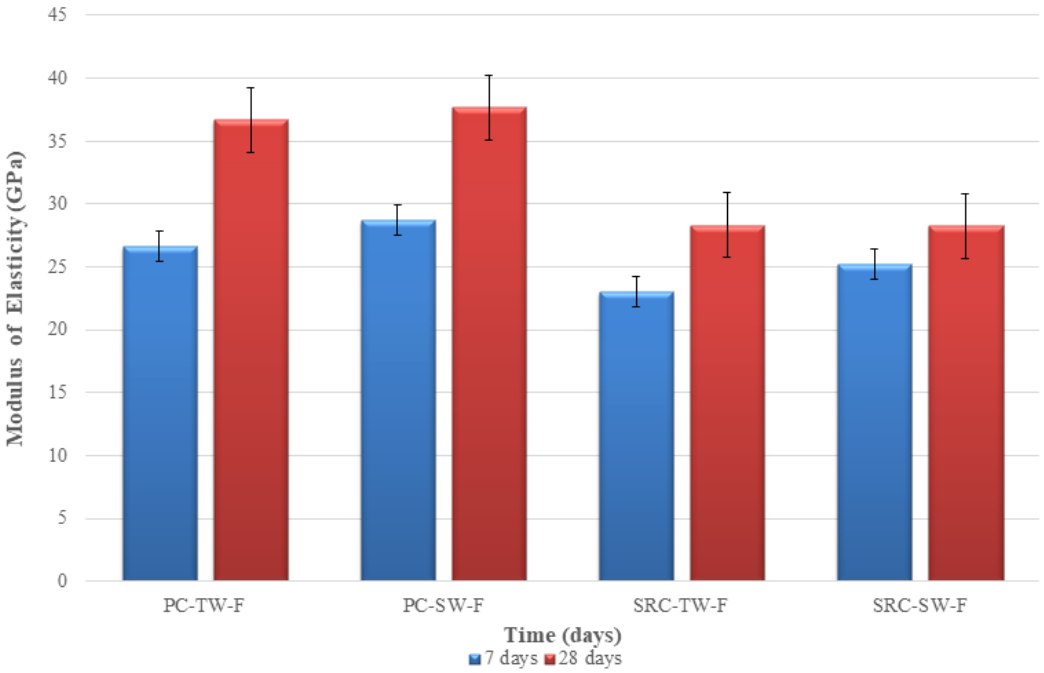

Figure 4.4. Modulus of elasticity of fibrous specimens

Results of modulus of elasticity tests were given in Figure 4.3 and Figure 4.4. When Figure 4.3 was examined, the results of non - fibrous specimens represent a tendency of decrease in modulus of elasticity values when seawater was used, on the other hand, the results of fibrous specimens represent a tendency of increase in modulus of elasticity values when seawater was used. However, these changes were not seem statistically significant when standard variation of the values were examined.

When literature was reviewed, Etxeberria *et al.* [14] reported that, the results of the modulus of elasticity of seawater achieved the highest value, this was the results of a higher development of the cement matrix hydration.

4.2.3. Three - Point Bending Test Results

Crack mouth opening displacement (CMOD) controlled three – point bending tests were performed on 3 prismatic notched specimens for each series at 28 days, and resulting load – CMOD graphs were given in Figure 4.6 and 4.7.

The area under force – CMOD curves represents toughness which is the energy absorption capacity of a material. The area under a curve was calculated by applying the method given in Figure 4.5.

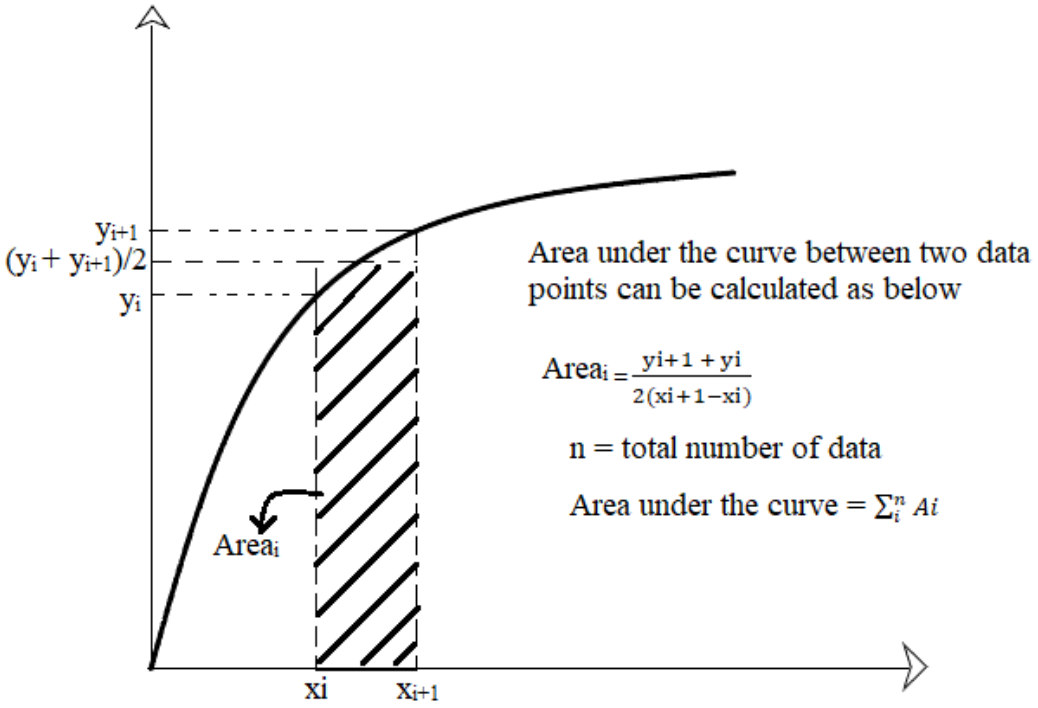

Figure 4.5. Calculation of area under the curve

Table 4.2. Toughness values of the non - fibrous specimens

Group	Specimen 1	Specimen 2	Specimen 3	Average (Nmm)
PC-TW-NF	1550	1369	1280	1400
PC-SW-NF	1574	1275	1455	1435
SRC-TW-NF	1287	1602	1567	1485
SRC-SW-NF	1756	1290	1283	1443

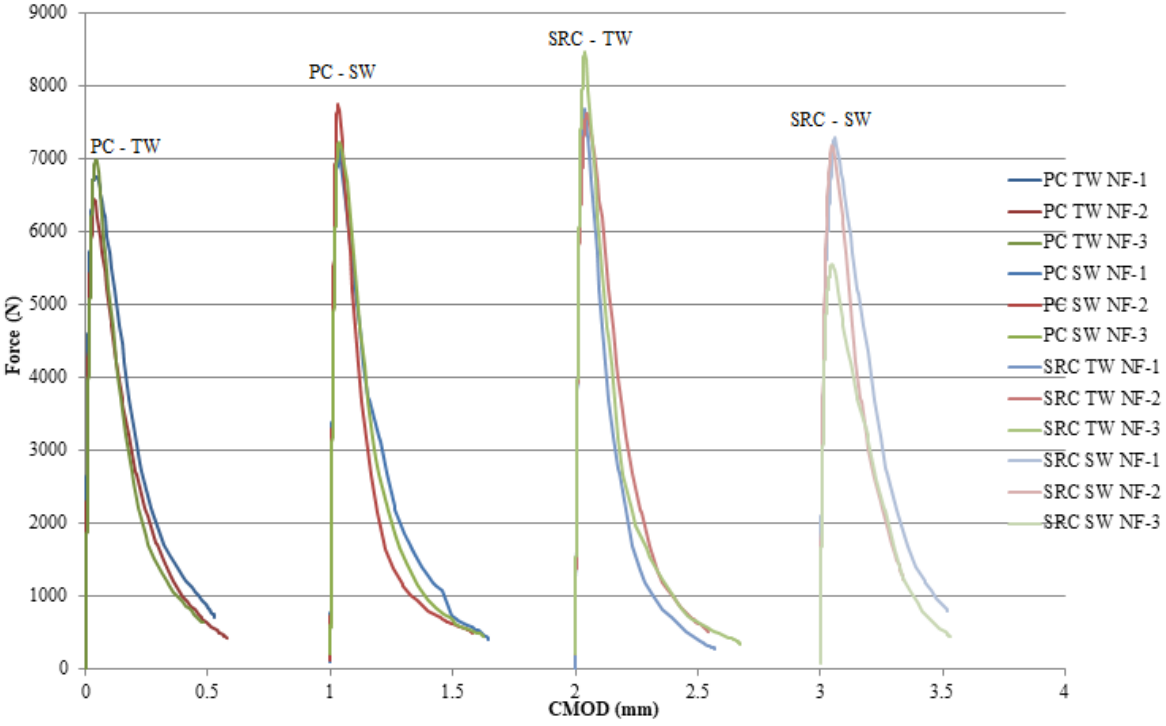

Figure 4.6. Force – CMOD graphs of non - fibrous specimens

As shown in Figure 4.6 and Table 4.2, when seawater was used in the non - fibrous mixtures, average toughness values were found to be very similar. However, when fibrous specimens when tested (Figure 4.7) the specimens cast by using tap water represented better mechanical performance. Toughness values were found to increase 41%, and 57% for PC and SRC made specimens, respectively.

Table 4.3. Toughness values of the fibrous specimens

Group	Specimen 1	Specimen 2	Specimen 3	Average (Nmm)
PC-TW-F	9838	5984	6308	7376
PC-SW-F	4853	6088	4672	5204
SRC-TW-F	7725	6744	6827	7098
SRC-SW-F	4319	4894	4265	4493

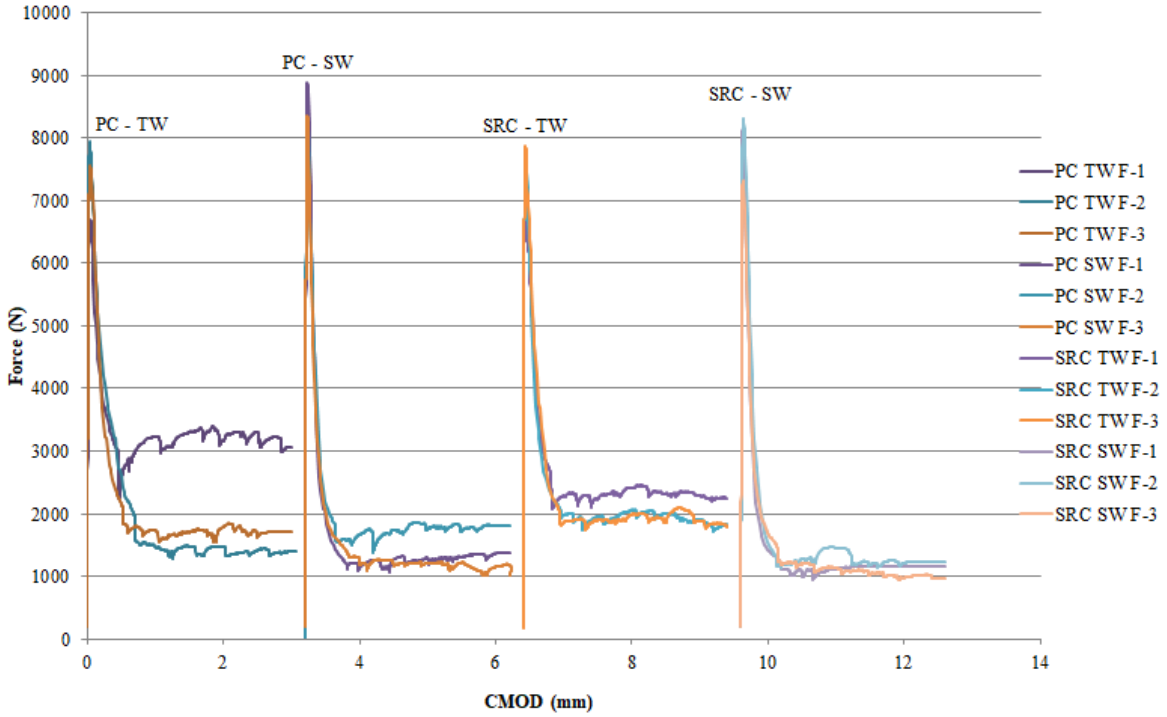

Figure 4.7. Force – CMOD graphs of fibrous specimens

When literature was reviewed, Wegian [5] reported that, concretes mixed and cured in seawater had higher flexural tensile strengths than concretes mixed and cured in fresh water in the early ages at 7 and 14 days. However, the strengths after 28 and 90 days for concrete mixes mixed and cured in fresh water increased in a gradual manner. According to Etxeberria *et al.* [14], the use of seawater produced similar flexural strength results to those of concretes produced with freshwater when using Portland cement. However, in the case of using blast - furnace slag cement, the flexural strength values of the seawater concretes increased by 5% on average in comparison to those of the flexural strength of the concretes mixed with freshwater. Younis *et al.* [2] said that, according to tensile strength test results, using seawater led to an initial slight increase until 7 days then to a decrease of approximately 10% at 28-day.

4.2.4. Length Change Test Results

Length change test was carried out the concrete mixtures based on ASTM-C157/C157M-17 [29]. At least 5 concrete prisms of each non – fibrous specimens (7.5 x 7.5 x 28.5 cm) were demolded and immersed in water for 30 minutes, then length measurements were taken. Samples were stored in the curing pool (23±2 °C). The length changes were measured at 28 days and calculated their ratio according to standard. These results might be seen in Figure 4.8.

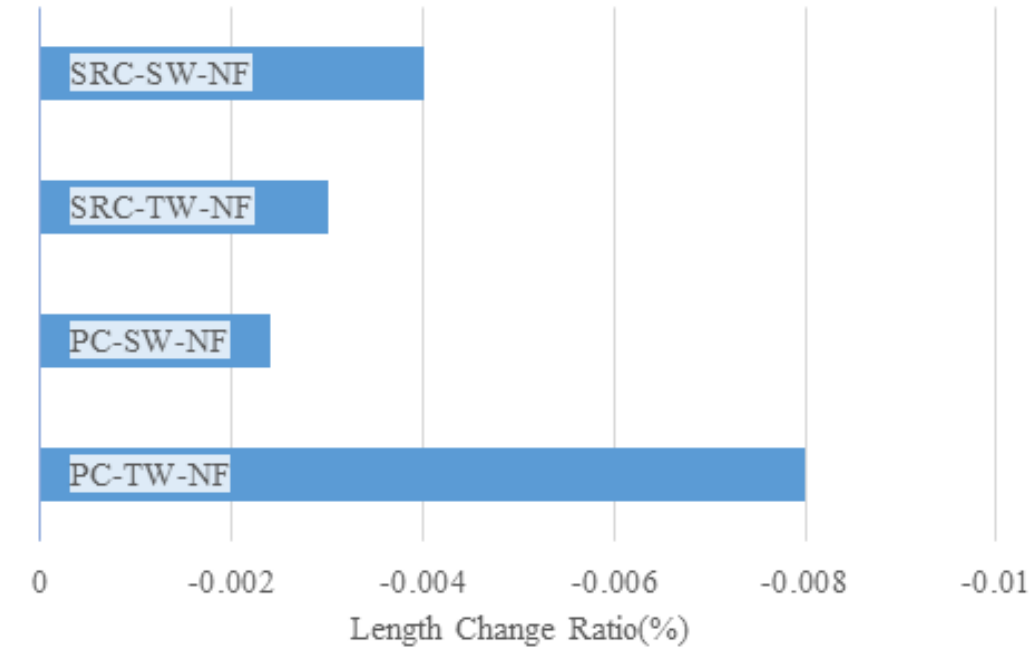

Figure 4.8. Length change ratio of non – fibrous specimens at 28 days

According to Figure 4.8, length change was found to be very small for all the specimens produced. The highest value was obtained when the specimens made by using portland cement and tap water.

4.2.5. SEM / EDAX Observations

SEM / EDAX observations was used to understand the morphological changes in the concrete. Samples were taken from both the surface and the center of the eight different beams and were prepared for the examination.

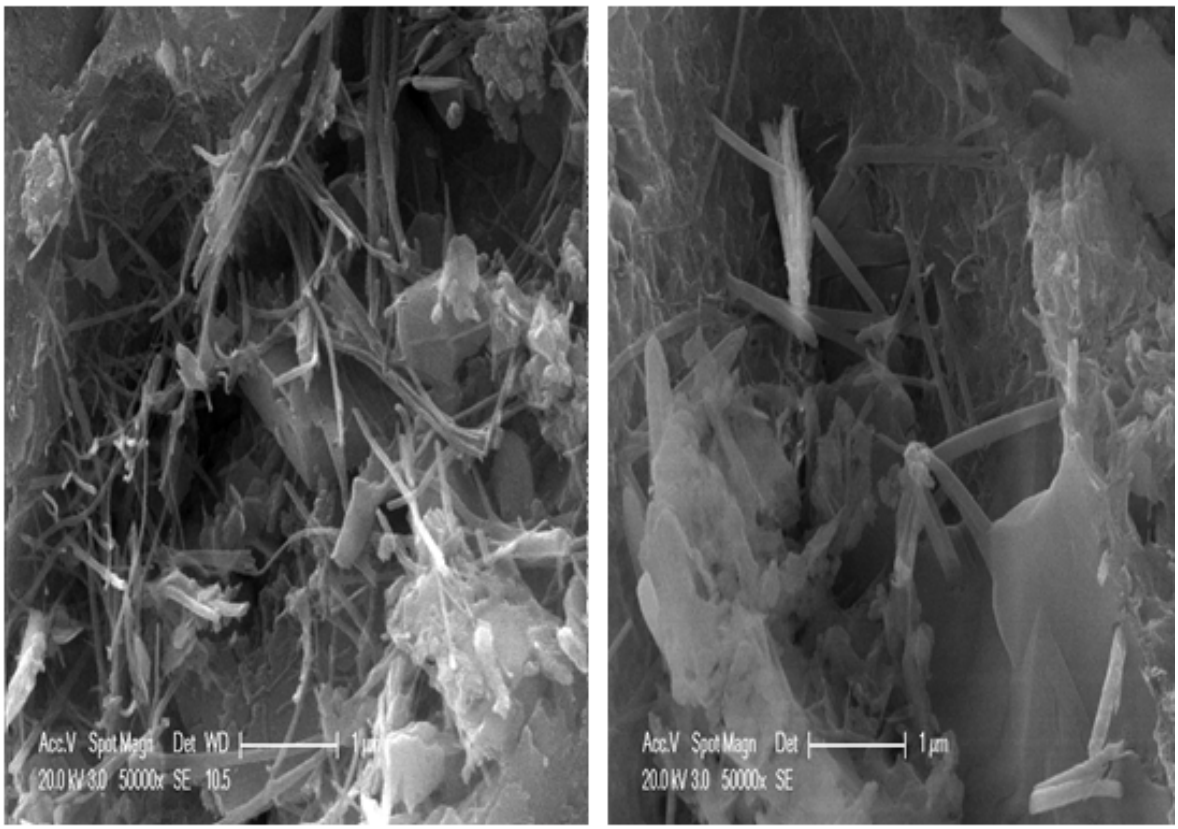

Figure 4.9. SEM images a) PC TW NF-surface, b) PC SW NF-surface

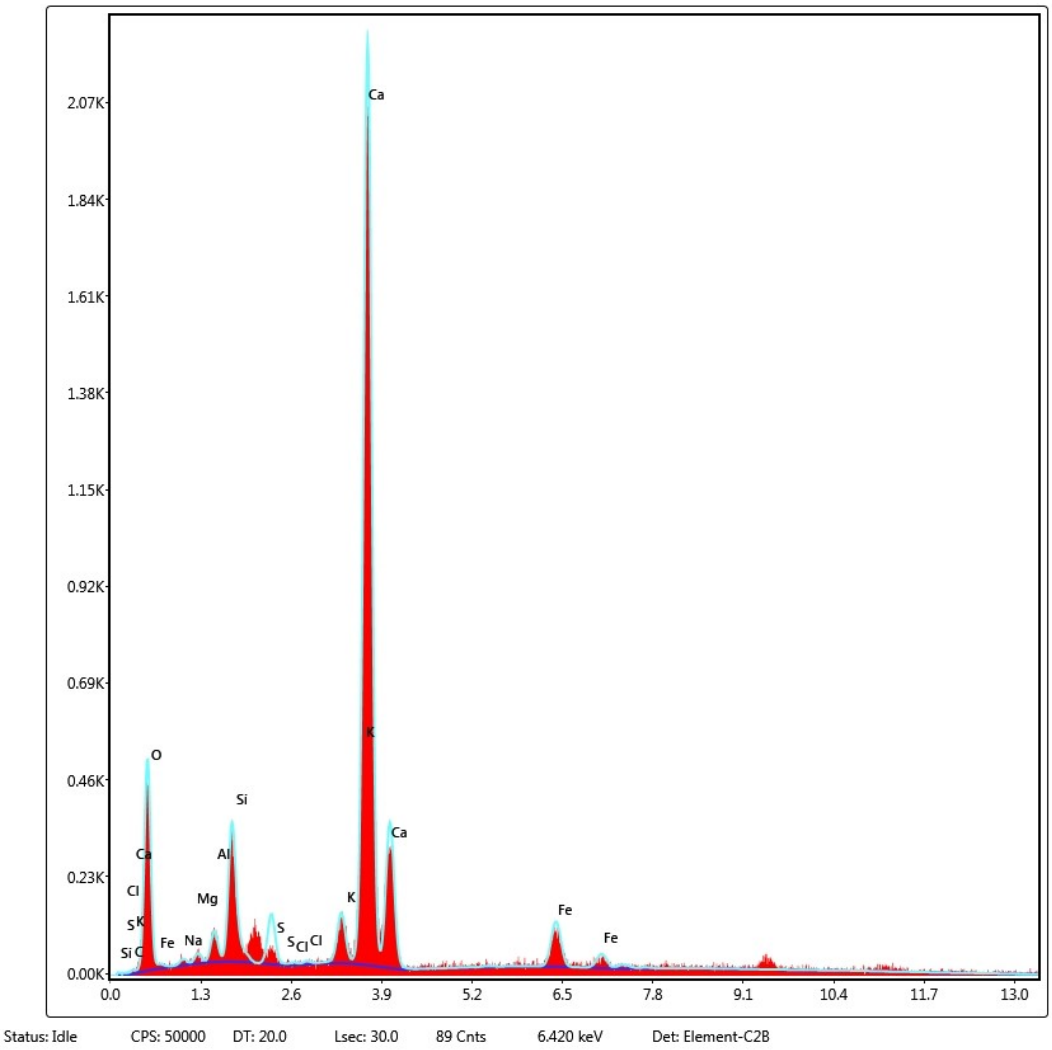

Figure 4.10. EDAX microanalysis for the PC TW NF

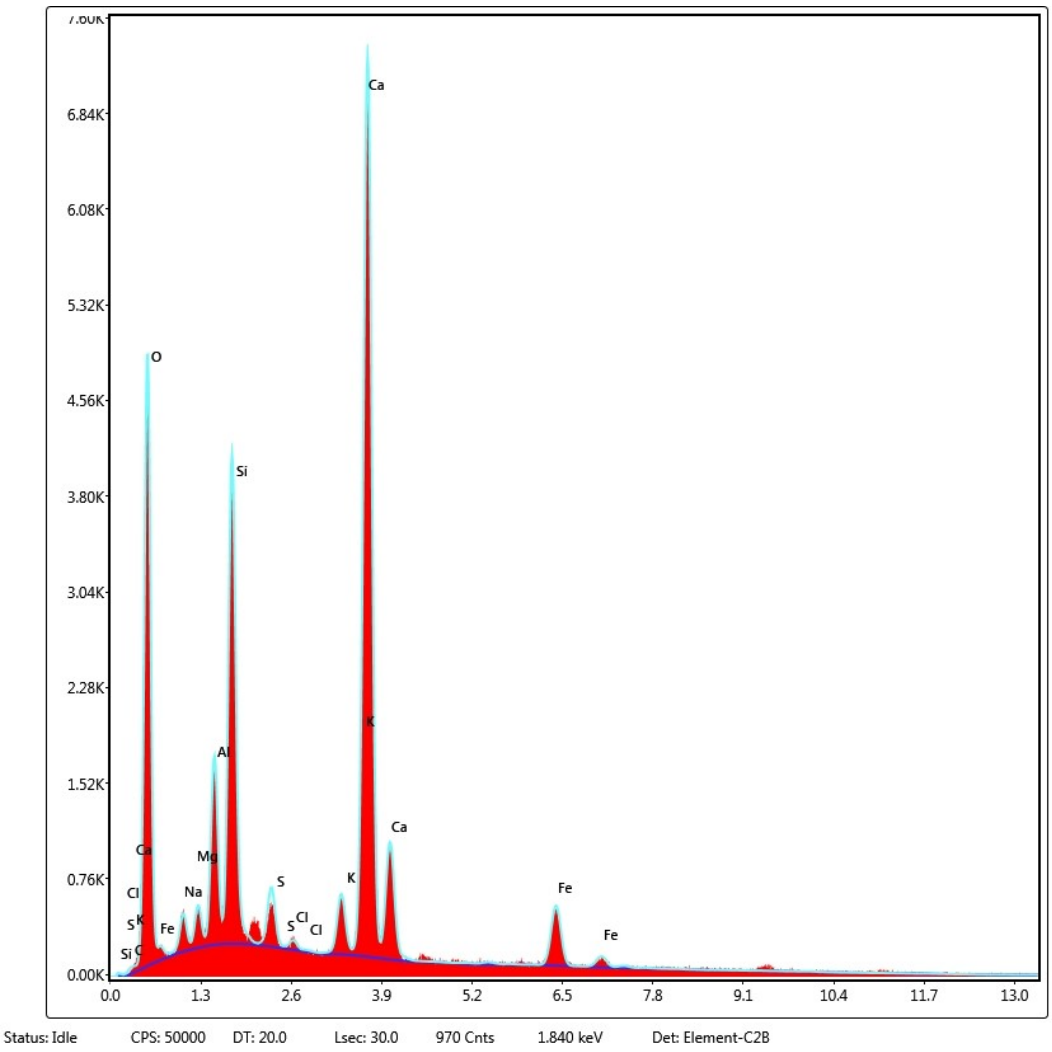

Figure 4.11. EDAX microanalysis for the PC SW NF

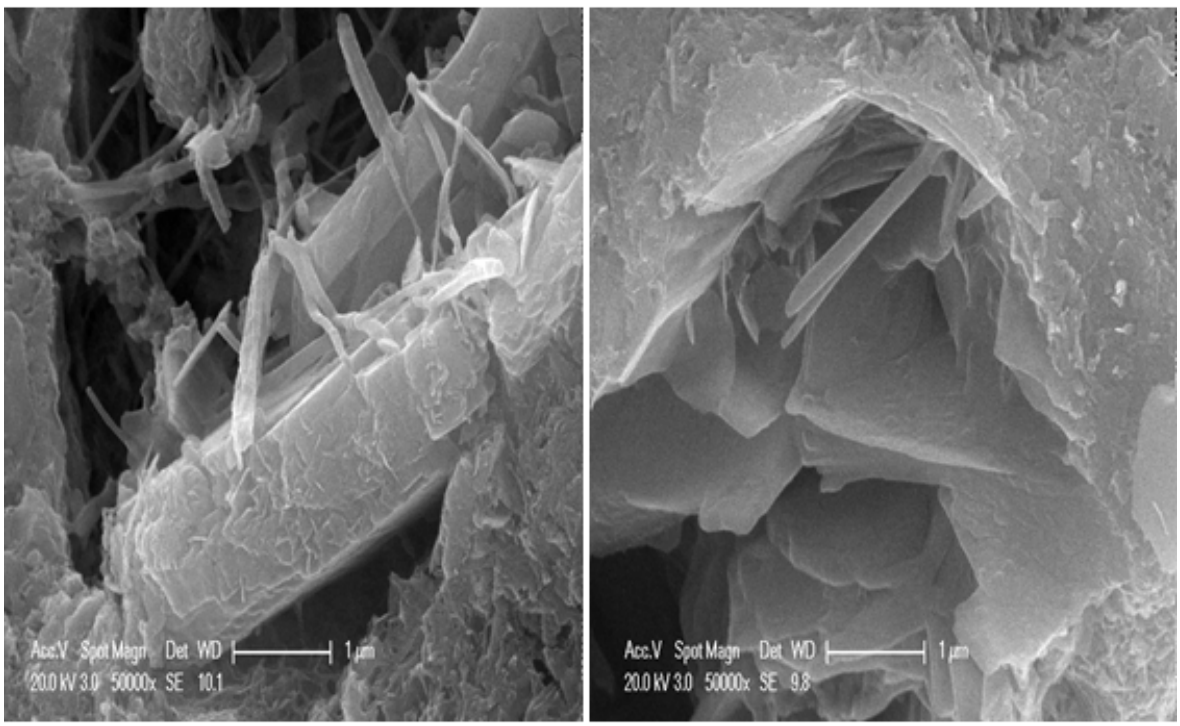

Figure 4.12. SEM images a) SRC TW NF-surface, b) SRC SW NF-surface

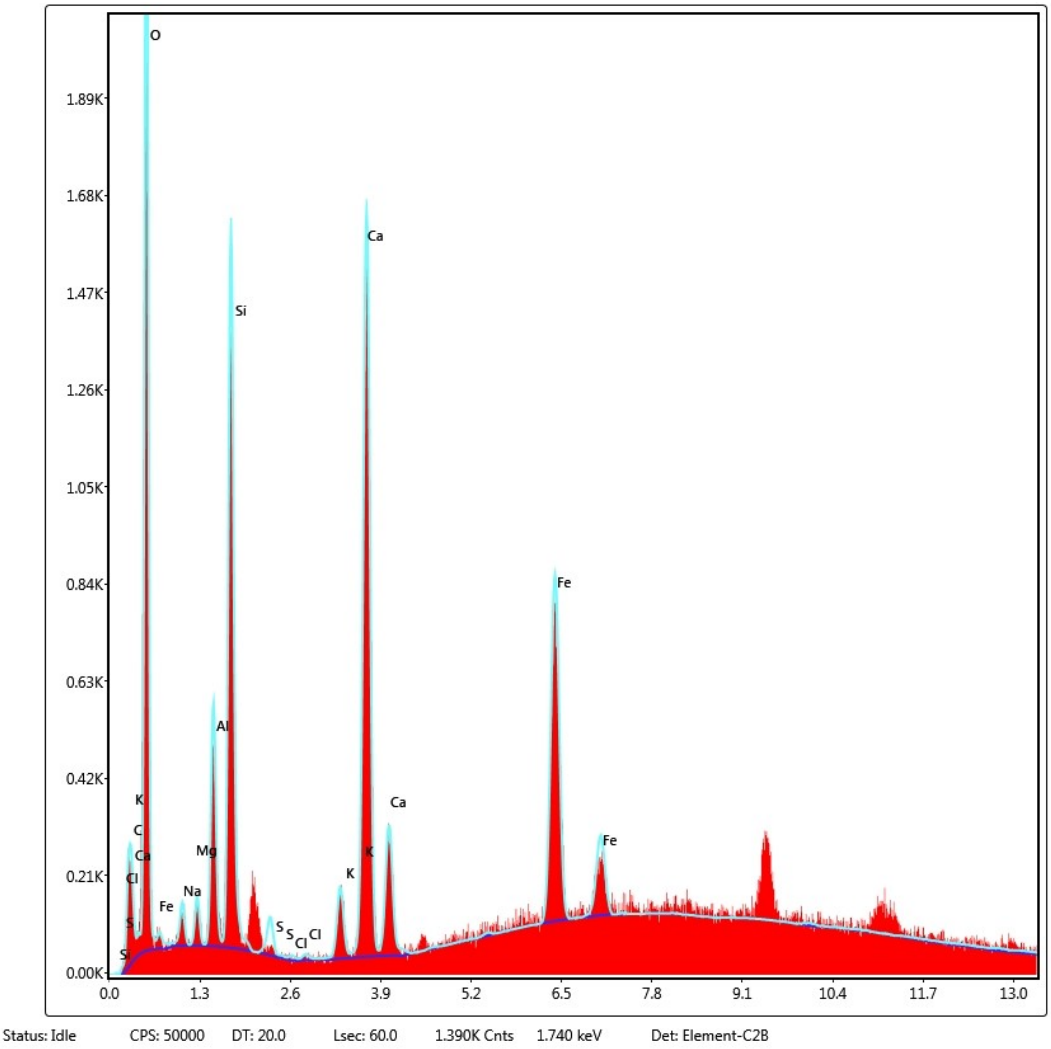

Figure 4.13. EDAX microanalysis for the SRC TW NF

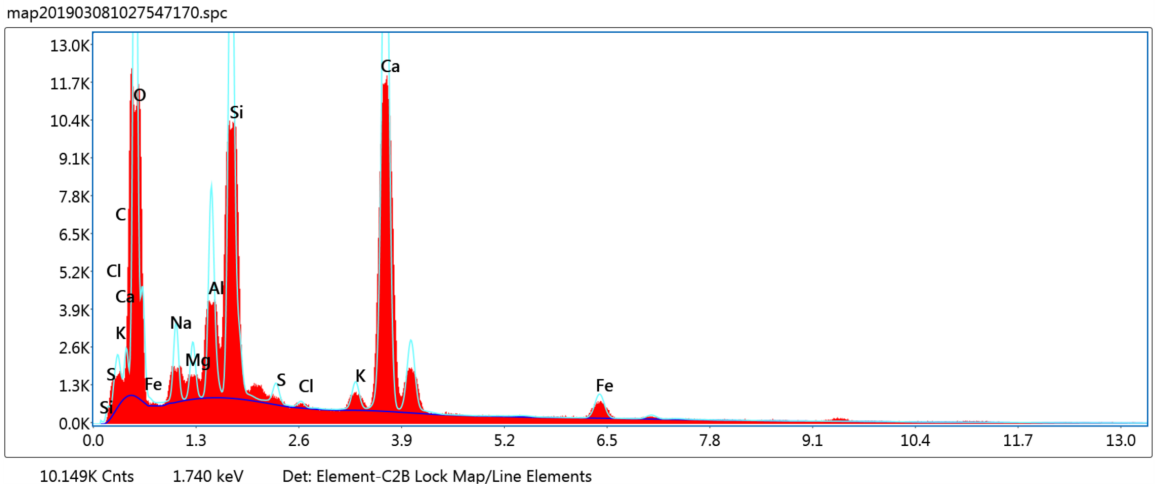

Figure 4.14. EDAX microanalysis for the SRC SW NF

Based on Figure 4.9, Figure 4.12, Figure 4.15 and 4.16, microstructure of the seawater paste revealed more densify than tap water paste [6]. According to conclusion of Figure 4.10, 4.11, 4.13 and 4.14, if the seawater is used as the mix water, amount of calcium (Ca) and oxygen (O) increase. It can be said that the amount of calcium hydroxide content ($Ca(OH)_2$, or CH in cement notation) increased in mixture containing seawater. Sodium (Na) and chlorine (Cl) atoms were also found in greater amounts in mixture containing seawater.

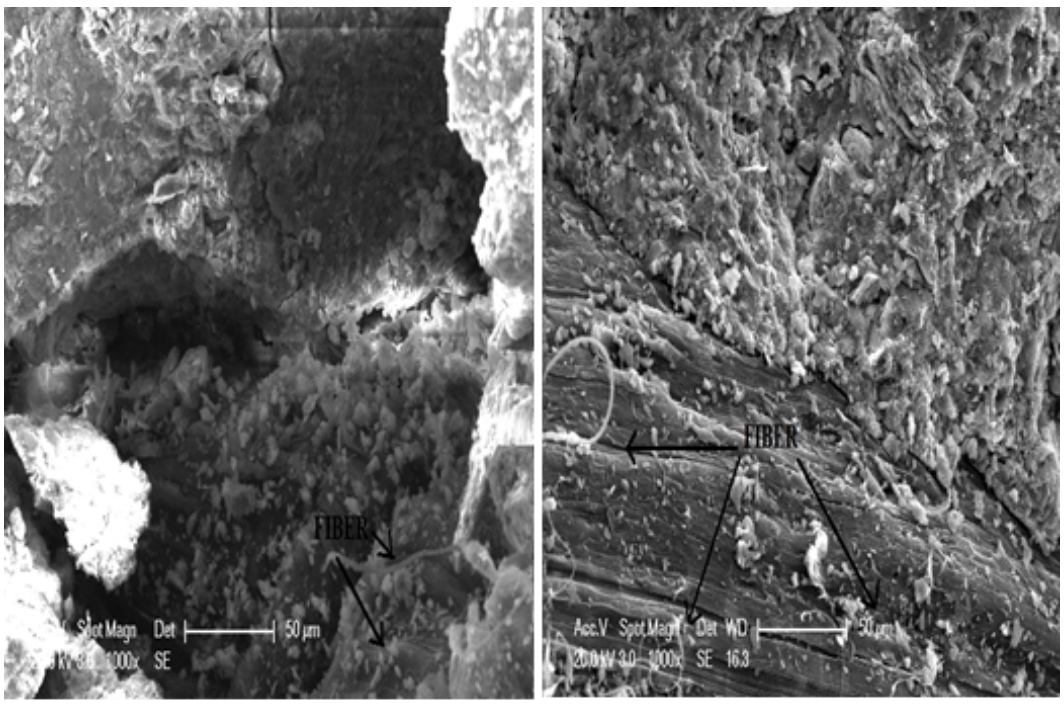

Figure 4.15. SEM images a) PC TW F, b) PC SW F

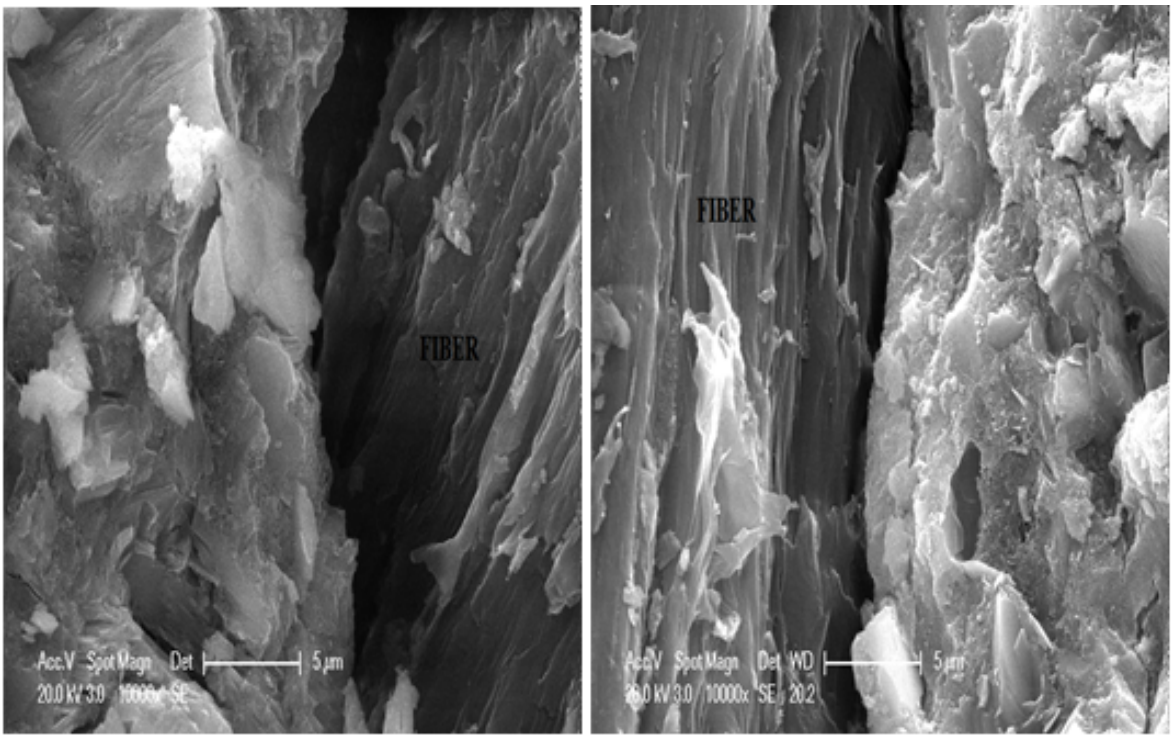

Figure 4.16. SEM images a) SRC TW F, b) SRC SW F

4.2.6. XRD Results

XRD results give information about the presence of phases and compounds in the pulverized sample. Specimens were taken from both the surface and the center of the four different non-fibrous beams. XRD results of samples obtained from non-fibrous beams might be seen from the following figures.

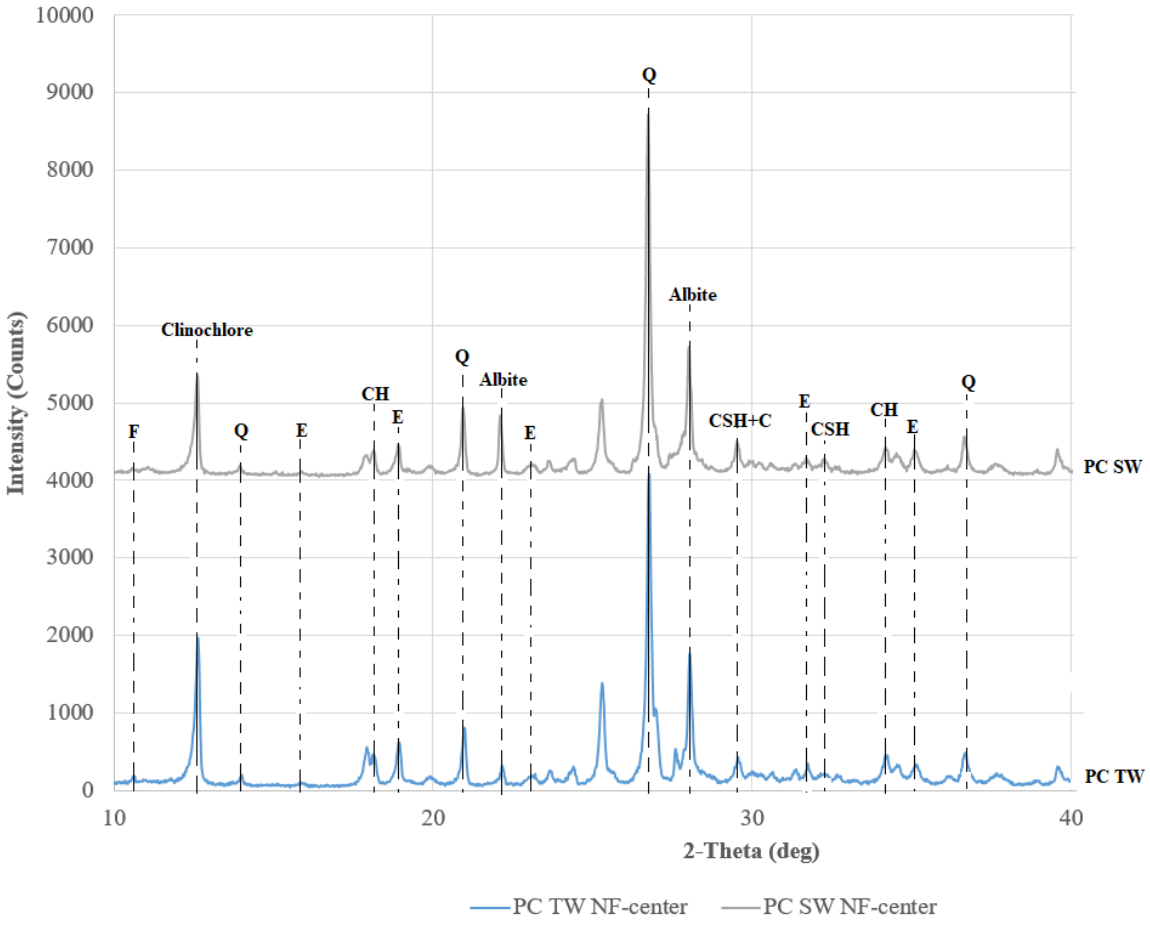

Figure 4.17. XRD results of center of the PC SW NF and PC TW NF specimens (F: Friedel's salt, Q: Quartz (SiO_2), E: Ettringite, CH: Portlandite ($Ca(OH)_2$), CSH: Calcium silicate hydrate, C: Calcite ($CaCO_3$), Albite ($NaAlSi_3O_8$), Clinochlore ($(Mg,Fe)6(Si,Al)4O10(OH)_8$))

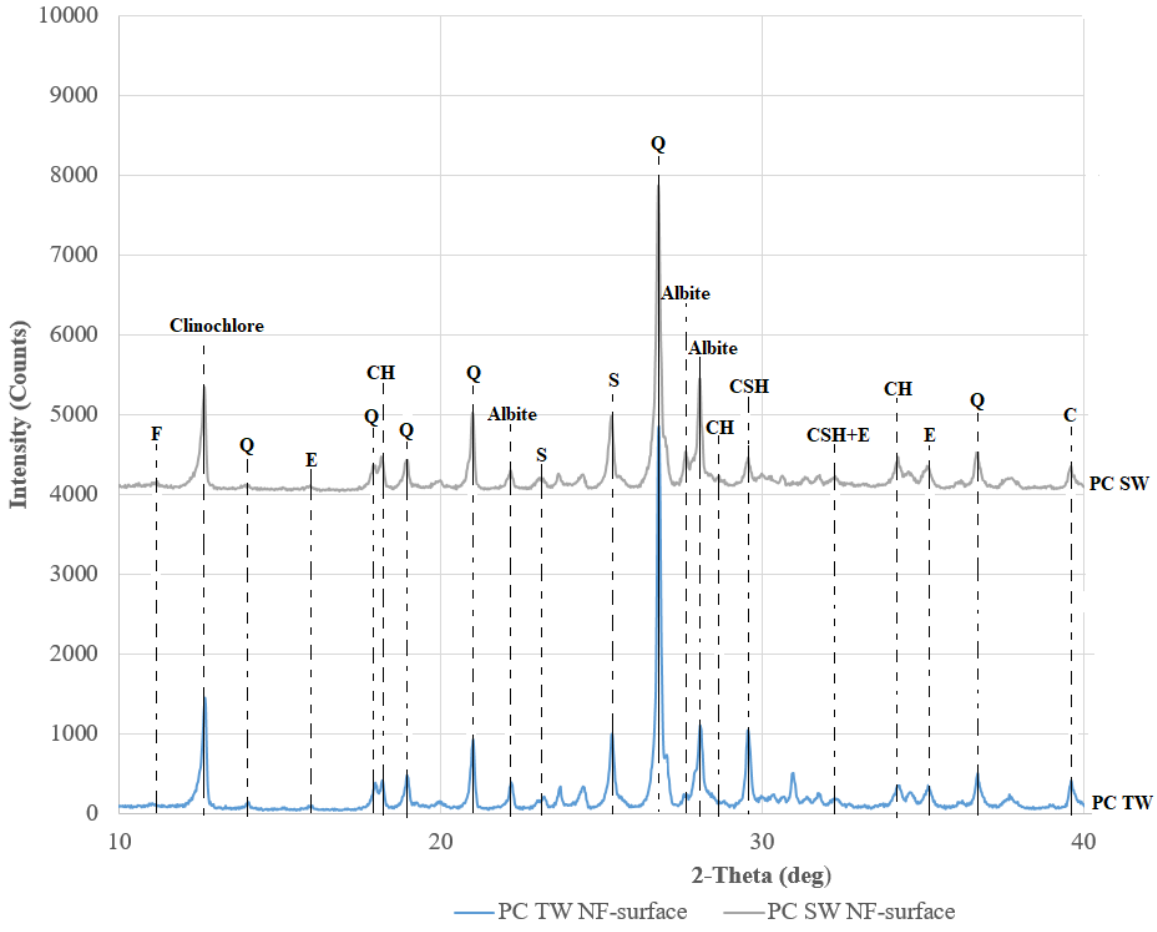

Figure 4.18. XRD results of surface of the PC SW NF and PC TW NF specimens (F: Friedel's salt, Q: Quartz , S: Calcium sulfate ($CaSO_4$), E: Ettringite, CH: Portlandite, CSH: Calcium silicate hydrate, C: Calcite, Albite ($NaAlSi_3O_8$), Clinochlore ((Mg,Fe)6(Si,Al)4O10(OH)$_8$))

According to Figure 4.17 and Figure 4.18, the ettringite formations ($Ca_6Al_2(SO_4)_3(OH)_{12}.25H_2O$) in concrete using seawater were almost similar than in concrete using tap water. Seawater also slightly increased calcium hydroxide content ($Ca(OH)_2$, or CH in cement notation) [9, 14]. Therefore, calcium silicate hydrates [30] ($3CaO.2SiO_2.3H_2O$, or C-S-H in cement notation) in concrete using seawater were nearly similar than in concrete using tap water. In addition, seawater increased Albite ($NaAlSi_3O_8$) compound because of presence of sodium in seawater. Seawater also slightly increased Friedel's salt formation ($C_3A.CaCl_2.H_{10}$) because of presence of calcium and chlorine in seawater.

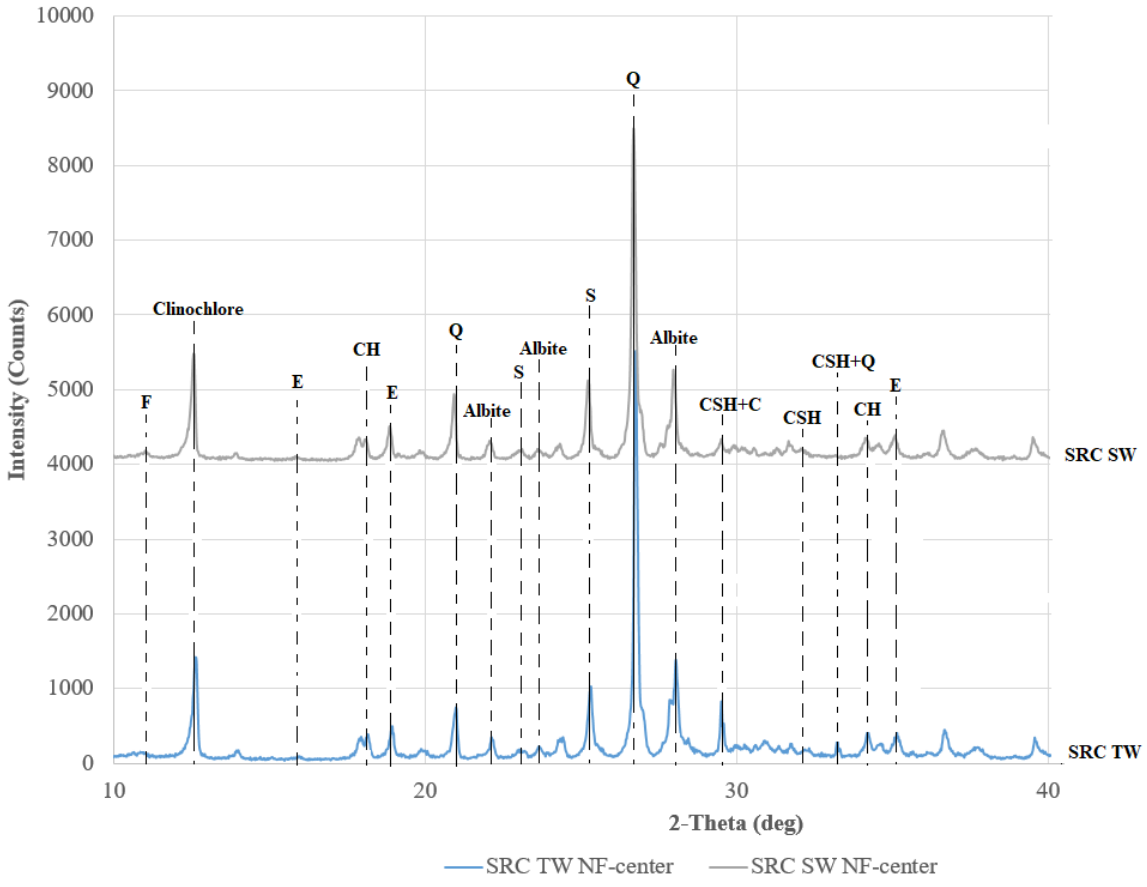

Figure 4.19. XRD results of center of the SRC SW NF and SRC TW NF specimens (F: Friedel's salt, Q: Quartz, S: Calcium sulfate, E: Ettringite, CH: Portlandite , CSH: Calcium silicate hydrate, C: Calcite, Albite ($NaAlSi_3O_8$), Clinochlore ($(Mg,Fe)6(Si,Al)4O10(OH)_8$))

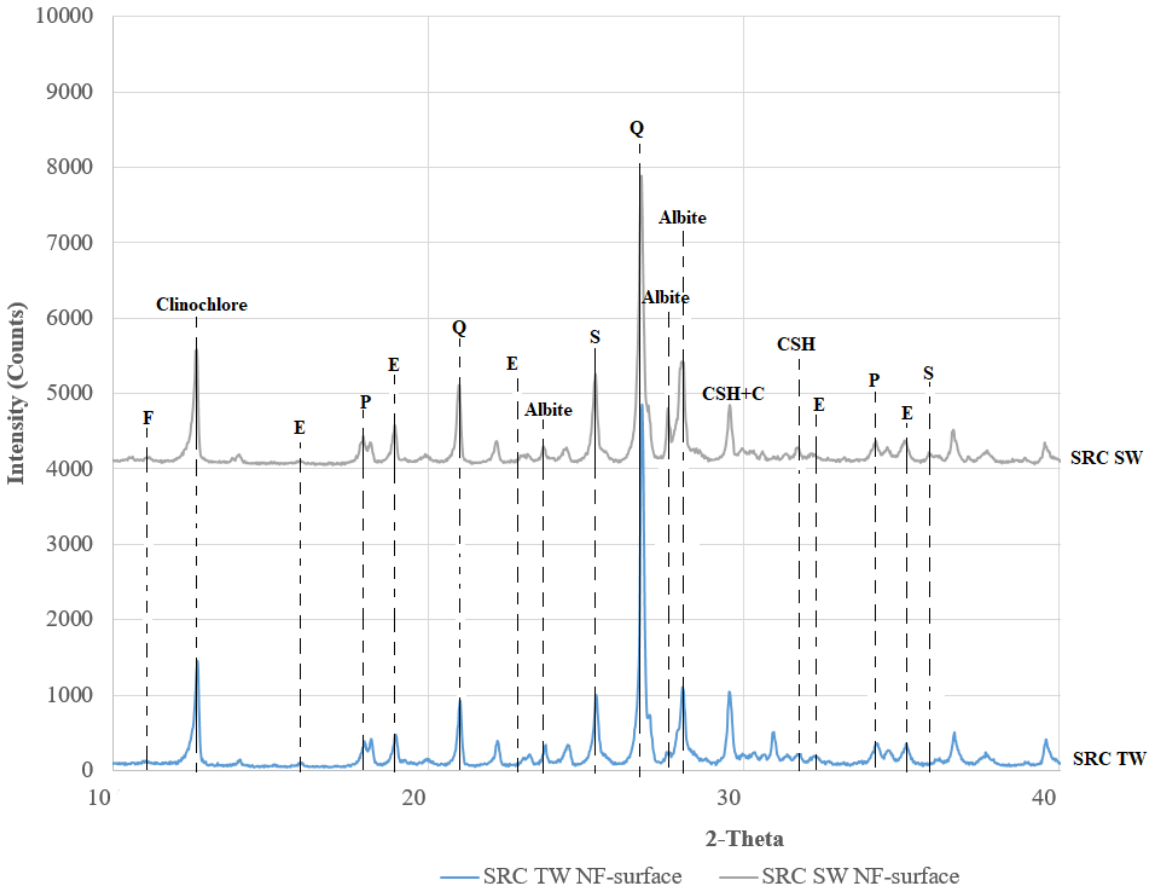

Figure 4.20. XRD results of surface of the SRC SW NF and SRC TW NF specimens (F: Friedel's salt, Q: Quartz (SiO_2), S: Calcium sulfate ($CaSO_4$), E: Ettringite, CH: Portlandite ($Ca(OH)_2$), CSH: Calcium silicate hydrate, C: Calcite ($CaCO_3$), Albite ($NaAlSi_3O_8$), Clinochlore ($(Mg,Fe)6(Si,Al)4O10(OH)_8$))

As shown in Figure 4.19 and Figure 4.20, aforementioned above, the ettringite formation and CH content in concrete using seawater were almost similar than in concrete using tap water. Albite compound, Friedel's salt and calcium sulfate were increased when the seawater was used in the mixture as mixing water. In addition, seawater increased Clinochlore compound ((Mg,Fe)6(Si,Al)4O10$(OH)_8$) because of presence of magnesium in seawater.

5. CONCLUSION

In this study, fresh and hardened properties of tap water and seawater-mixed concretes were compared and the following were found:

(i) Almost all mixes had similar slump values, ranging between 17-21 cm, and densities, ranging between 2410-2441 kg/m^3.

(ii) Compressive strength was decreased when seawater was used in non – fibrous mixtures. However, no significant effect on compressive strength was seen when seawater was used in fibrous mix.

(iii) The results of fibrous specimens represent a tendency of increase in modulus of elasticity values when seawater was used, on the other hand, non - fibrous specimens represent a tendency of decrease in modulus of elasticity values.

(iv) When seawater was used in the non - fibrous mixtures, no significant change was observed in three – point bending behavior. Average toughness values were found to be very similar. However, when fibrous specimens when tested the specimens cast by using tap water represented better mechanical performance. Toughness values were found to increase 41%, and 57% for PC and SRC made specimens, respectively.

(v) Length change was found to be very small for all the specimens produced. The highest value was obtained when the specimens made by using portland cement and tap water.

(vi) Based on SEM / EDAX observations, many needle crystals of ettringite were formed in the pores of concrete mixed using seawater. These crystals filling large voids densified the microstructure. When seawater was used in the mixtures, amount of calcium (Ca) and oxygen (O) increase. So that, the amount of calcium hydroxide content ($Ca(OH)_2$, or CH in cement notation) increased.

(vii) According to XRD results, the ettringite formations in both non – fibrous and fibrous concrete using seawater were almost similar than in concrete using tap water. Seawater also slightly increased calcium hydroxide content. Therefore, calcium silicate hydrates in concrete using seawater were nearly similar than in concrete using tap water. In addition, seawater increased Albite compound because of presence of sodium in seawater. Seawater also slightly increased Friedel's salt formation because of presence of calcium and chlorine in seawater. In addition, seawater increased Clinochlore compound because of presence of magnesium in seawater.

REFERENCES

1. The United Nations World Water Development Report 2018, *Nature-Based Solutions for Water*, 2018.

2. Younis, A., U. Ebead, P. Suraneni and A. Nanni, "Fresh and hardened properties of seawater-mixed concrete", *Construction and Building Materials*, Vol. 190, pp. 276–286, 2018.

3. Nishida, T., N. Otsuki, H. Ohara, Z. M. Garba-Say and T. Nagata, "Some considerations for applicability of seawater as mixing water in concrete", *Journal of Materials in Civil engineering*, Vol. 27, No. 7, p. B4014004, 2013.

4. Mohammed, T. U., H. Hamada and T. Yamaji, "Performance of seawater-mixed concrete in the tidal environment", *Cement and concrete research*, Vol. 34, No. 4, pp. 593–601, 2004.

5. Wegian, F. M., "Effect of seawater for mixing and curing on structural concrete", *The IES Journal Part A: Civil & Structural Engineering*, Vol. 3, No. 4, pp. 235–243, 2010.

6. Katano, K., N. Takeda, Y. Ishizeki and K. Iriya, "Properties and application of concrete made with sea water and un-washed sea sand", *Proceedings of Third International conference on Sustainable Construction Materials and Technologies*, 2013.

7. Otsuki, N., T. Nishida, C. Yi, T. Nagata and H. Ohara, "Effect of blast furnace slag powder and fly ash on durability of concrete mixed with seawater", *4th International Conference on the Durability of Concrete Structures*, 2014.

8. Bhaskar, S., S. M. S. and E. John, "Relevance of sea water as mixing water in concrete", *International Journal of Innovative Research in Science, Engineering*

and Technology, Vol. 5, pp. 17084–17090, 2016.

9. Shi, Z., Z. Shui, Q. Li and H. Geng, "Combined effect of metakaolin and sea water on performance and microstructures of concrete", *Construction and Building Materials*, Vol. 74, pp. 57–64, 2015.

10. Li, Q., H. Geng, Z. Shui and Y. Huang, "Effect of metakaolin addition and seawater mixing on the properties and hydration of concrete", *Applied Clay Science*, Vol. 115, pp. 51–60, 2015.

11. Şahmaran, Mustafa, *Deterioration Mechanisms – Chemical*, Thomas Telford Limited, 2010.

12. Fallah, S. and M. Nematzadeh, "Mechanical properties and durability of high-strength concrete containing macro-polymeric and polypropylene fibers with nano-silica and silica fume", *Construction and building materials*, Vol. 132, pp. 170–187, 2017.

13. Hasan-Nattaj, F. and M. Nematzadeh, "The effect of forta-ferro and steel fibers on mechanical properties of high-strength concrete with and without silica fume and nano-silica", *Construction and Building Materials*, Vol. 137, pp. 557–572, 2017.

14. Etxeberria, M., A. Gonzalez-Corominas and P. Pardo, "Influence of seawater and blast furnace cement employment on recycled aggregate concretes' properties", *Construction and Building Materials*, Vol. 115, pp. 496–505, 2016.

15. Bertola, F., F. Canonico and A. Nanni, "SEACON Project: sustainable concrete using seawater, salt-contaminated aggregates, and non-corrosive reinforcement", *XIV DBMC-14th International Conference on Durability of Building Materials and Components*, 2017.

16. Standards Institute, T., *TS 802 Design of Concrete Mixes*, 2009.

17. Standards Institute, T., *TS 6228 EN ISO 7980 - Su kalitesi - Kalsiyum ve magnezyum tayini -Atomik absorpsiyon spektrometrik metot*, 2002.

18. Standards Institute, T., *SM 4110- Standard methods fort he examination of water and wastewater*, 1992.

19. Standards Institute, T., *TS 4164 ISO 9297- Su kalitesi - Klorür tayini - Kromat indikatörü yanında gümüş nitrat ile titrasyon (Mohr metodu)*, 1992.

20. Standards Institute, T., *TS 5095- Methods for the analysis of water - Determination of sulfate content - Turbidimetric method*, 2013.

21. Standards Institute, T., *TS EN 1008- Mixing water for concrete – Specification for sampling, testing and assessing the suitability of water, including water recovered from processes in the concrete industry, as mixing water for concrete*, 2003.

22. Standards Institute, T., *TS EN ISO 10523- Water quality - Determination of pH*, 2013.

23. Standards Institute, T., *TS EN 12390-2 Beton - Sertleşmiş beton deneyleri - Bölüm 2: Dayanım deneylerinde kullanılacak deney numunelerininin yapımı ve küre tâbi tutulması*, 2002.

24. Standards Institute, T., *TS EN 12350-2- Testing fresh concrete - Part 2: Slump test*, 2002.

25. Standards Institute, T., *BS EN 12390-3 Testing hardened concrete - Compressive strength of test specimens*, 2009.

26. Standards Institute, T., *BS EN 12390-13 Determination of secant modulus of elasticity in compression*, 2013.

27. Concrete Institute Standard, J., *JCI-S-001 Method of test for fracture energy of concrete by use of notched beam*, 2003.

28. Concrete Institute Standard, J., *JCI-S-002 Method of test for load-displacement curve of fiber reinforced concrete by use of notched beam*, 2003.

29. International, A., *ASTM C157 - Standard test method for length change of hardened hydraulic-cement mortar and concrete*, 2017.

30. Mendes, A., W. P. Gates, J. G. Sanjayan and F. Collins, "NMR, XRD, IR and synchrotron NEXAFS spectroscopic studies of OPC and OPC/slag cement paste hydrates", *Materials and structures*, Vol. 44, No. 10, pp. 1773–1791, 2011.